Gen. Physiol. Biophys. (2023), **42,** 1–12

doi: 10.4149/gpb_2022050

Immune-based prognostic biomarkers associated with metastasis of osteosarcoma

Teng Ma, Changliang Peng, Dongjin Wu, Song Yang, Li Ji, Zhang Cheng and Chunzheng Gao

Department of Spine Surgery, The Second Hospital of Shandong University, Shandong University, Jinan, China

Abstract. This study aimed to identify immune-based prognostic biomarkers associated with metastasis of osteosarcoma. Based on the GEO and TCGA databases, 437 differentially expressed genes were screened between primary and metastatic osteosarcoma. Weighted gene co-expression network analysis (WGCNA) revealed 496 genes in turquoise module which had the highest correlation with osteosarcoma metastasis. Within these two group genes, 122 common genes involved in osteosarcoma metastasis were identified. These genes were enriched in chemokine activity, chemokine receptor binding, TNF signaling pathway, etc. Survival analysis revealed 8 prognostic genes (ANK3, EGR1, FBP1, FOS, KIFC3, MAOB, ISLR and MFAP4) from the 122 genes. RT-qPCR showed that all of these eight genes were differentially expressed between 143B and MNNG/HOS Cl cells. Various infiltrating immune cells showed significant differences between primary and metastatic osteosarcoma. Expression of all the 8 prognostic genes was correlated with infiltration abundance of multiple immune cells, such as follicular helper T cells, activated dendritic cells. In addition, 10 microRNAs and 7 transcription factors that targeted these prognostic genes were predicted. In conclusion, 8 immune-based prognostic genes associated with osteosarcoma metastasis were identified.

Key words: Osteosarcoma — Metastasis — Infiltrating immune cells — Biomarker — Prognosis

Abbreviations: DEGs, differentially expressed genes; GO, Gene Ontology; MDSC, marrow derived suppressor cells; ORA, over-representation analysis; TFs, transcription factor; TIICs, tumor-infiltrating immune cells; TME, tumor microenvironment; WGCNA, weighted gene co-expression network analysis.

Introduction

Osteosarcoma is the most common primary bone malignant tumor originated from mesenchymal tissue, usually occurring in adolescents aged 10~20 years, also showing a second peak of incidence in elderly individuals (Eaton et al. 2021). Osteosarcomas tend to develop mainly in long tubular epiphyses with abundant blood supply. Clinically, osteosarcoma presents only with local pain and swelling, with occasional joint dysfunction (Gianferante et al. 2017). Osteosarcoma has a high propensity for local invasion and metastasis, with the most common sites of metastasis being lung (over 85%) and bone (Lilienthal et al. 2020). Although remarkable achievements have been made in the treatment of osteosarcoma in a multidisciplinary framework, with an improved 5-year survival rate reaching to 60–70% (Harrison et al. 2018; Lilienthal et al. 2020). However, patients with recurrent or metastatic osteosarcoma still have a poor prognosis, with 5-year survival rate less than 30% (Sayles

---

Electronic supplementary material. The online version of this article (doi: 10.4149/gpb_2022050) contains Supplementary material.

Correspondence to: Chunzheng Gao, Department of Spine Surgery, The Second Hospital of Shandong University, Shandong University, 247 Beiyuan Street, Jinan, Shandong, China, 250033
E-mail: gaochunzheng1964@sina.com

et al. 2019). Hence, it's necessary to develop more effective therapeutics to improve the prognosis for recurrent or metastatic osteosarcoma.

Immunotherapy has achieved great efficacy in the treatment of various human tumors, and enhances to the understanding of immune response in osteosarcoma in recent years (Chen et al. 2021). Chemotherapy commonly used for osteosarcoma (doxorubicin, cisplatin, and alkylating agents) activates immune effector cells by killing immunosuppressive regulatory T cells and bone marrow derived suppressor cells (MDSC) to induce immune-antitumor activity (Zitvogel et al. 2008). In children with osteosarcoma, lymphocyte count is positively associated with good prognosis after chemotherapy (Moore et al. 2010). This indicates that immunotherapy may have great potential for the treatment of metastatic and recurrent osteosarcoma. On the other hand, tumor microenvironment (TME) has been proven to be closely associated with the initiation and development of tumors by regulating tumor growth and cell extravasation, of which immune infiltrate consists one of these tumor niches (Heymann et al. 2019; Luo et al. 2020). Being a group of main non-tumor cellular populations within TME, tumor-infiltrating immune cells (TIICs) have proven to show close correlations with the prognosis and response to treatments (Tas et al. 2017; Farhood et al. 2019; Garaud et al. 2019; Wang et al. 2019). For example, Chen et al. (2020) indicated that monocytes and naive B cells in osteosarcoma was correlated with worse survival, and established a reliable and effective risk model based on the 8 TIICs to predict survival for osteosarcoma. These findings indicated that the development and application of immune-related predictive biomarkers had great potential in osteosarcoma.

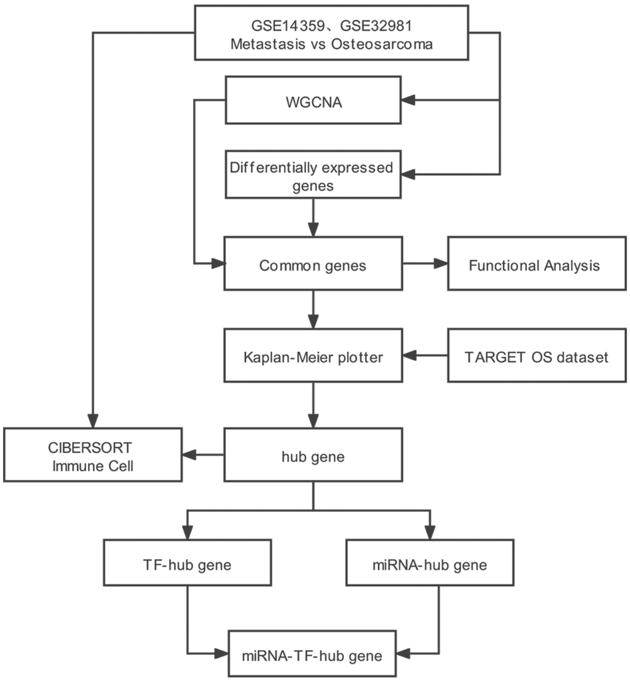

Figure 1. The workflow of this study.

TME may have different influences during diverse stages of development and metastasis of osteosarcoma by considering the heterogeneity and complexity of cells within TME (Liu et al. 2021). In this study, several immune-based prognostic genes associated with osteosarcoma metastasis were identified. Additionally, the microRNAs (miRNAs) and transcription factor (TF) that targeted these immune-based prognostic genes were explored. This study will provide potential biomarkers and targets for the treatment of metastatic osteosarcoma.

Materials and Methods

Data acquisition and preprocessing

The preprocessed and standardized probe expression matrix of osteosarcoma samples in GSE14359 dataset and GSE32981 dataset were downloaded from the Gene Expression Omnibus database (http://www.ncbi.nlm.nih.gov/geo/). The osteosarcoma samples in these two datasets were assigned into two groups of primary osteosarcoma tissue samples or metastatic tissue samples. The 10 osteosarcoma tissue samples and 8 metastatic tissue samples in GSE14359 dataset (GPL96 [HG-U133A] Affymetrix Human Genome U133A Array platform), and 12 osteosarcoma tissue samples and 11 metastatic tissue samples in GSE32981 dataset (GPL3307 ABI Human Genome Survey Microarray v2.0 platform) were used in this study. Genes were annotated based on the annotation files provided by corresponding platforms. Probes matching no gene symbol were removed, and the mean value was considered as the final expression value when multiple probes matching to the same gene symbol. Then, based on the expression matrix of the common genes, these two microarray datasets were merged as one dataset after eliminating batch effect using ComBat function in sva package (version 3.34.0) in R.

Additionally, the log2(fpkm+1) expression data, overall survival and clinical phenotype data of 70 osteosarcoma samples in TARGET dataset were downloaded from University of California Santa Cruz Xena browser (https://xenabrowser.net/), including 67 osteosarcoma tissue samples and 8 metastatic tissue samples. All the data were analyzed as *per* the workflow shown in Figure 1.

Differential expression analysis

Differentially expressed genes (DEGs) between metastatic tissue samples and primary osteosarcoma tissue samples were screened using the classical Bayesian method provided by Limma package (version 3.10.3) in R with the threshold value of $|\text{logFC}|>0.263$ (1.2-fold change) and Benjamini & Hochberg multiple test corrected $p < 0.05$.

Weighted gene co-expression network analysis

Based on the calculation principle of weighted gene co-expression network analysis (WGCNA), genes that highly-coexpressed in one module can be regarded as a set of specifically expressed genes of a certain type of cells in tumor tissues. Genes with the absolute deviation of median expression ranked in top 2000 from all the genes were used to perform WGCNA analysis *via* "WGCNA" package (version 1.61) in R. First, the adjacency matrix weight parameter power value was determined to balance the relationship within mean connectivity and scale independence, followed by the determination of intergenic diverging coefficients. Cluster dendrogram was then constructed to display the gene clusters. In order to identify the gene modules significantly associated with osteosarcoma and metastatic phenotype, gene significance for each module was calculated to compute module-trait relationships.

Then, the overlapped genes between DEGs and phenotype-associated module genes were screened with VENN analysis using VennDiagram package (version 1.6.20) in R, and the screened overlapped genes were used in following analyses.

Functional enrichment analysis

The Gene Ontology (GO) annotations and pathways enrichment analysis were performed using over-representation analysis (ORA) method provided in Functional profiling module of g profiler online tool (https://biit.cs.ut.ee/gprofiler/convert). GO annotations consist of biological process, cellular component and molecular function terms, and pathways consist of Reactome pathway and KEGG pathway. Benjamini & Hochberg multiple test corrected $p < 0.05$ was used as cut-off value.

Screening of prognostic genes using survival analysis

Using the expression data and clinical data from TARGET database, the samples were assigned into high-expression and low-expression groups according to median expression value of genes to perform survival analysis. Prognostic genes were identified with $p < 0.05$.

Characterization of immune infiltration

The infiltration abundance of 22 immune cells for all samples in merged microarray datasets were estimated by using CIBERSORT deconvolution algorithm based on the LM22 gene expression characteristic provided in CIBERSORT website with parameters setting as perm = 100 and QN = F. The differences on infiltration abundance of each immune cell type between metastatic tissue samples and primary osteosarcoma tissue samples were compared using WilcoxTest with the significant threshold of $p < 0.05$. The vioplot package (version 0.3.5) in R was used to draw violin plot.

Correlation analysis between prognostic genes and immune infiltration

In order to determine the correlations between prognostic genes and differential immune infiltration cells, Pearson correlation coefficient was calculated, followed by correlation test. $p < 0.05$ was used to present significant correlations.

Prediction of transcription factor and miRNA for prognostic genes

The miRNAs that target prognostic genes were predicted using miRWalk 3.0 (http://zmf.umm.uni-heidelberg.de/apps/zmf/mirwalk3.html) to obtain miRNA-target gene pairs. The miRNA-target pairs with score > 0.9 and existed in both miRDB (http://www.mirdb.org/miRDB/download.html) and miRTarBase (http://mirtarbase.cuhk.edu.cn/php/index.php) databases were selected. Then, TF that regulates prognostic genes was predicted using TRRUST online tool (https://www.grnpedia.org/trrust/) to obtain TF-target gene pairs. Finally, the TF-target gene pairs and miRNA-target gene pairs were integrated to construct regulatory network.

Literature search for prognostic genes

GenCLiP 3.0 database (http://ci.smu.edu.cn/GenCLiP3/analysis.php#) was used to summarize literatures related to prognostic genes that involved in osteosarcoma.

RT-qPCR

RT-qPCR was performed to validate the expression of prognostic genes in Human osteosarcoma cell line MNNG/HOS Cl (low aggressive) and 143B cell line (high aggressive). In brief, total RNA was isolated from cells utilizing TRIZOL reagent (catalog No. CW0580; CWBIO, China), followed by the determination of RNA concentration. The cDNA was synthesized firstly by reverse transcription using a HiFiScript cDNA Synthesis Kit (catalog No. CW2569; CWBIO, China). Next, RT-qPCR was performed using UltraSYBR Mixture (catalog No. CW0957; CWBIO, China) on a PCR Amplifier (H9800, Suzhou Hehui Biotechnology Co., LTD). The primer sequences are listed in Supplementary material, Table S1.

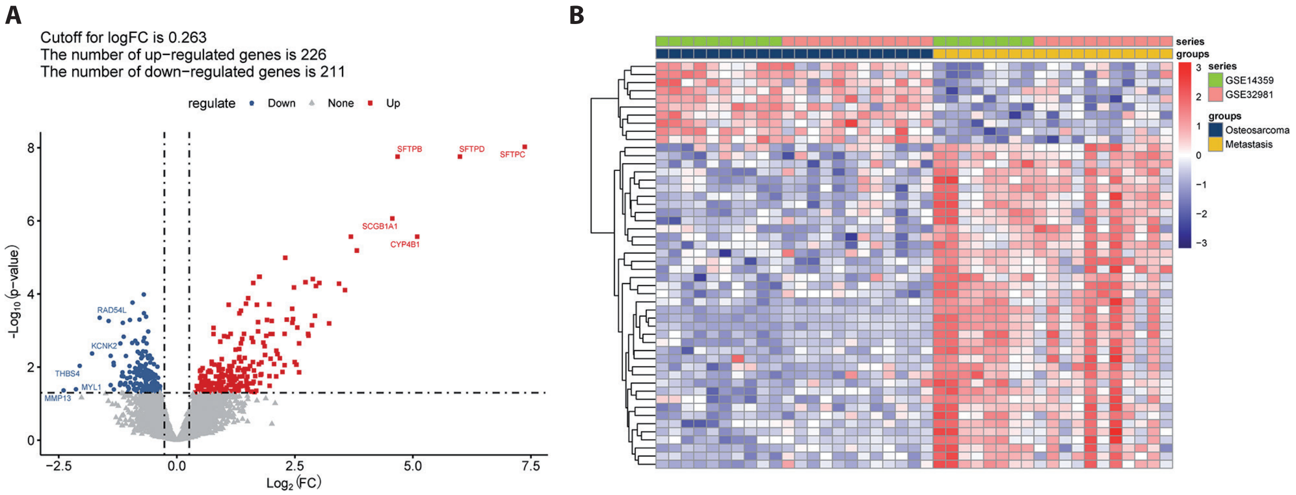

Figure 2. Differential expression analysis. **A.** Volcano plot of differentially expressed genes. Red and blue dots represent up-regulated and down-regulated genes, respectively. **B.** Heatmap of differentially expressed genes. (See online version for color figure.)

Table 1. Correlation of immune infiltration with prognostic genes

Genes	Immune cells	*p* value	Cor. value
ISLR	T cells CD4 memory resting	0.032910231	0.3338465
ISLR	Macrophages M0	0.002377221	-0.461692
ISLR	Dendritic cells activated	0.000206786	0.548219
MFAP4	T cells CD8	0.019498885	0.3634644
MFAP4	T cells CD4 memory resting	0.011786505	0.3896843
MFAP4	T cells regulatory (Tregs)	0.0388575	-0.32387
MFAP4	T cells gamma delta	0.019455569	-0.363585
MFAP4	Macrophages M0	0.000197605	-0.549628
MFAP4	Dendritic cells resting	0.000340843	0.5322851
MFAP4	Dendritic cells activated	0.001339969	0.4841411
MAOB	Macrophages M0	0.03817301	-0.324952
MAOB	Dendritic cells resting	0.017030781	0.3707158
MAOB	Dendritic cells activated	0.028331111	0.342595
EGR1	T cells regulatory (Tregs)	0.013568279	-0.382554
EGR1	Dendritic cells resting	0.004157361	0.4382558
EGR1	Dendritic cells activated	0.002172206	0.4653252
FOS	T cells CD8	0.009979156	0.3979256
FOS	Macrophages M0	0.002641949	-0.457388
FOS	Dendritic cells resting	0.000307198	0.5356648
FOS	Dendritic cells activated	0.000298866	0.5365531
FOS	Eosinophils	0.048928168	0.3095133
FBP1	T cells CD8	0.003199469	0.4494402
FBP1	Macrophages M0	0.000673853	-0.509199
FBP1	Dendritic cells resting	1.72E-05	0.6171768
FBP1	Dendritic cells activated	0.003069811	0.4511734
FBP1	Mast cells activated	0.034155126	0.3316425
ANK3	T cells follicular helper	0.014625416	0.3786921
ANK3	Dendritic cells resting	0.017396419	0.3695879

Cor. value: Pearson correlation coefficient.

Statistical analysis

Data for RT-qPCR was presented as mean ± standard deviation (SD). Expression of prognostic genes in MNNG/HOS Cl (low aggressive) and 143B (low aggressive) cells was compared using *t*-test provided by Graphpad prism 5 (Graphpad Software, San Diego, CA). $p < 0.05$ indicates statistical significance.

Results

Genes differentially expressed between primary and metastatic osteosarcoma

Differential expression analysis between primary and metastatic osteosarcoma samples revealed 437 DEGs with the cutoff value of $|\text{logFC}| > 0.263$ and $p < 0.05$, of which 226 genes were up-regulated while 211 genes were down-regulated (Fig. 2A, Table S2). These DEGs could obviously distinguish the primary and metastatic osteosarcoma samples (Fig. 2B).

Identification of osteosarcoma and metastatic phenotype associated gene module

To explore the possible connections among genes, we performed WGCNA analysis to identify gene modules with similar genes expression patterns. The soft threshold power of 9 (no scale $R^2 = 0.9$) was selected to construct an approximate scale-free network (Fig. 3A). Cluster dendrogram was constructed with the minimum number of genes in each gene module setting as 30, and the cut height setting as 0.3, and 9 gene modules were obtained (Fig. 3B). Figure 3C showed the correlations between the gene significance of each module and the disease status (osteosarcoma and metastasis), of which turquoise module had the highest correlation with disease status. In order to ensure the reliability of turquoise module as disease status-significantly associated module, absolute value of gene significance of each module was calculated to compute module-trait relationships (Fig. 3D). The turquoise module had the highest correlation with disease status ($|r| = 0.7$ and $p < 0.05$). Therefore, 496 genes in turquoise module were selected.

Functional enrichment analysis

Between the 437 DEGs and the 496 genes in turquoise module, VENN analysis revealed 122 overlapped genes (Fig. 4A). These 122 overlapped genes were considered as important genes that involved in the progression of osteosarcoma metastasis. In order to further explore the biological functions and pathways of these genes, enrichment analysis was performed. Figure 4B and C showed the top 5 enriched terms of each category. It could be seen that these genes were implicated in biological processes such as response to external stimulus and response to chemical, and in molecular functions such as chemokine activity and chemokine receptor binding (Fig. 4B). Additionally, these genes were enriched in nuclear events (kinase and transcription factor activation), TNF signaling pathway, IL-17 signaling pathway, etc. (Fig. 4C).

Identification of prognostic genes

Survival analysis was performed to investigate the prognostic value of these important genes involved in the pro-

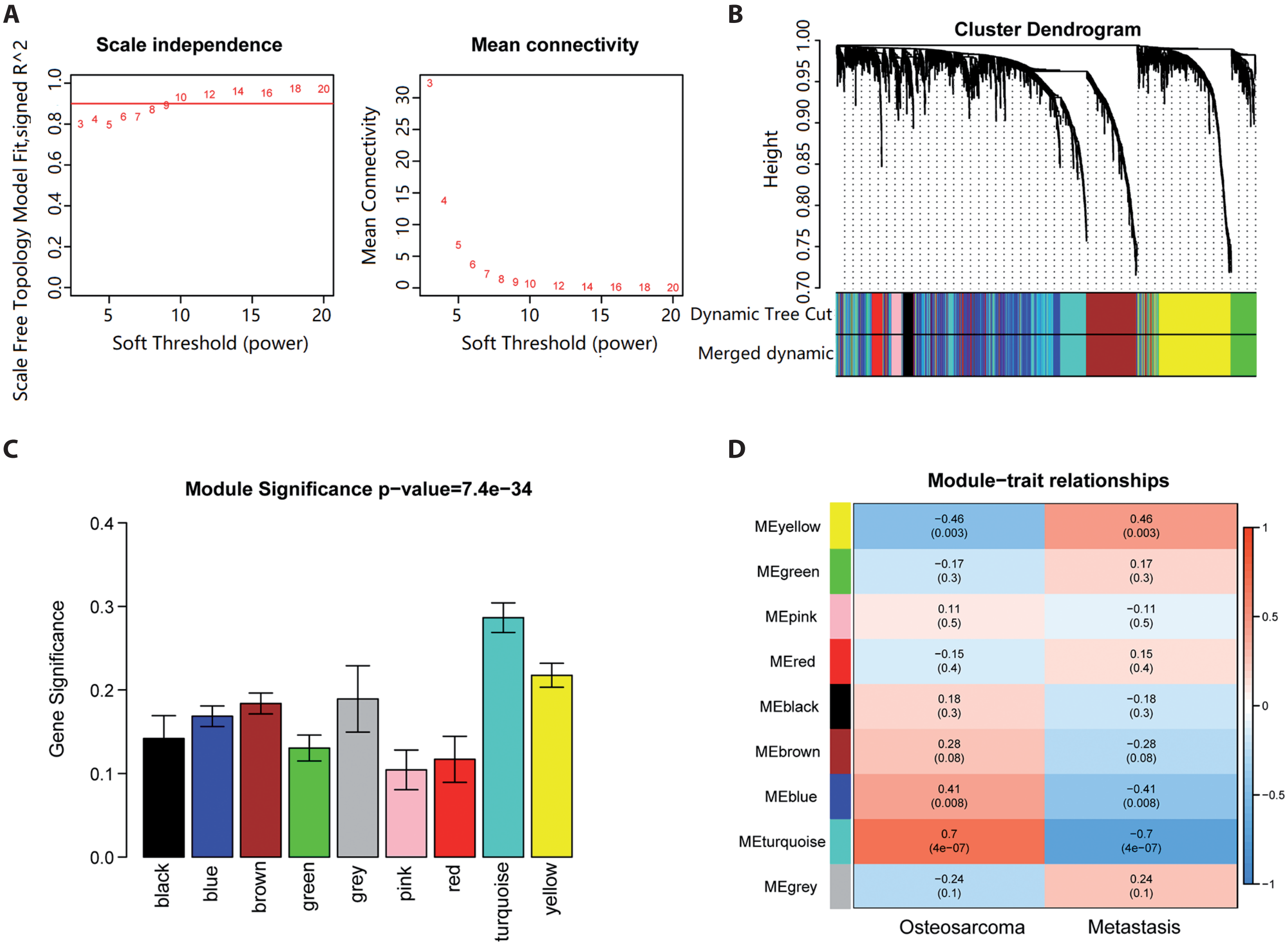

Figure 3. Weighted gene co-expression network analysis. **A.** Network topology for different soft-threshold powers. The scale independence (left) and mean connectivity (right) for various soft-threshold powers. **B.** Cluster dendrogram was obtained by hierarchical clustering. Each color branches represent a color-coded module containing a highly interconnected set of genes. **C.** Disease status correlated co-expression modules. x-axis represents different gene modules, and y-axis represents the overall correlation coefficient between genes in each module and disease status. **D.** Module-trait relationships and p values for selected traits (osteosarcoma and metastasis).

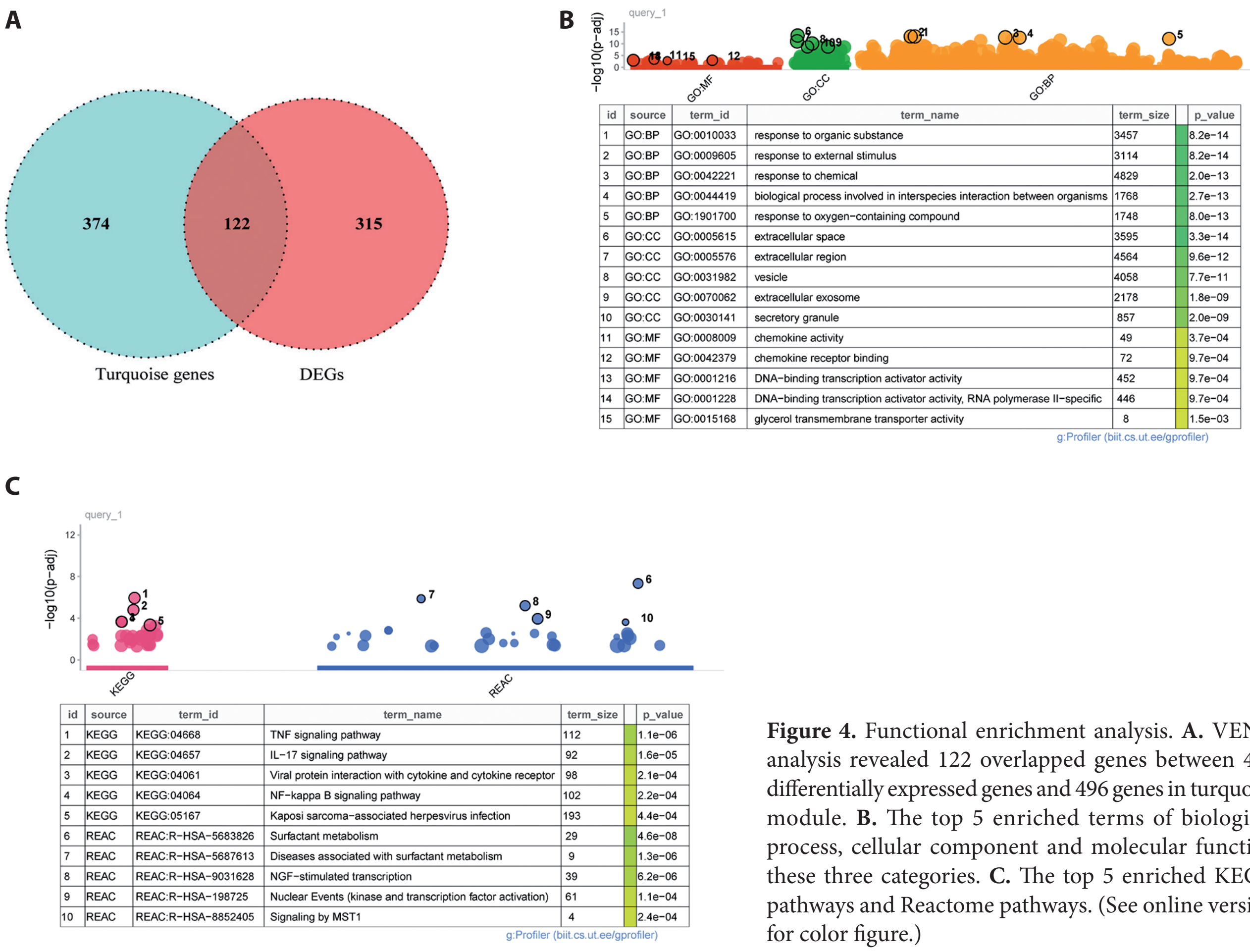

id	source	term_id	term_name	term_size		p_value
1	GO:BP	GO:0010033	response to organic substance	3457	🟩	8.2e−14
2	GO:BP	GO:0009605	response to external stimulus	3114	🟩	8.2e−14
3	GO:BP	GO:0042221	response to chemical	4829	🟩	2.0e−13
4	GO:BP	GO:0044419	biological process involved in interspecies interaction between organisms	1768	🟩	2.7e−13
5	GO:BP	GO:1901700	response to oxygen−containing compound	1748	🟩	8.0e−13
6	GO:CC	GO:0005615	extracellular space	3595	🟩	3.3e−14
7	GO:CC	GO:0005576	extracellular region	4564	🟩	9.6e−12
8	GO:CC	GO:0031982	vesicle	4058	🟩	7.7e−11
9	GO:CC	GO:0070062	extracellular exosome	2178	🟩	1.8e−09
10	GO:CC	GO:0030141	secretory granule	857	🟩	2.0e−09
11	GO:MF	GO:0008009	chemokine activity	49	🟨	3.7e−04
12	GO:MF	GO:0042379	chemokine receptor binding	72	🟨	9.7e−04
13	GO:MF	GO:0001216	DNA−binding transcription activator activity	452	🟨	9.7e−04
14	GO:MF	GO:0001228	DNA−binding transcription activator activity, RNA polymerase II−specific	446	🟨	9.7e−04
15	GO:MF	GO:0015168	glycerol transmembrane transporter activity	8	🟨	1.5e−03

g:Profiler (biit.cs.ut.ee/gprofiler)

id	source	term_id	term_name	term_size		p_value
1	KEGG	KEGG:04668	TNF signaling pathway	112	🟩	1.1e−06
2	KEGG	KEGG:04657	IL−17 signaling pathway	92	🟨	1.6e−05
3	KEGG	KEGG:04061	Viral protein interaction with cytokine and cytokine receptor	98	🟨	2.1e−04
4	KEGG	KEGG:04064	NF−kappa B signaling pathway	102	🟨	2.2e−04
5	KEGG	KEGG:05167	Kaposi sarcoma−associated herpesvirus infection	193	🟨	4.4e−04
6	REAC	REAC:R−HSA−5683826	Surfactant metabolism	29	🟩	4.6e−08
7	REAC	REAC:R−HSA−5687613	Diseases associated with surfactant metabolism	9	🟩	1.3e−06
8	REAC	REAC:R−HSA−9031628	NGF−stimulated transcription	39	🟩	6.2e−06
9	REAC	REAC:R−HSA−198725	Nuclear Events (kinase and transcription factor activation)	61	🟨	1.1e−04
10	REAC	REAC:R−HSA−8852405	Signaling by MST1	4	🟨	2.4e−04

g:Profiler (biit.cs.ut.ee/gprofiler)

Figure 4. Functional enrichment analysis. **A.** VENN analysis revealed 122 overlapped genes between 437 differentially expressed genes and 496 genes in turquoise module. **B.** The top 5 enriched terms of biological process, cellular component and molecular function these three categories. **C.** The top 5 enriched KEGG pathways and Reactome pathways. (See online version for color figure.)

gression of osteosarcoma metastasis (the 122 overlapped genes). Based on their median expression value, samples were assigned into high-expression and low-expression groups to investigate the differences on overall survival. As shown in Figure 5, 8 prognostic genes were found. Of which, high expression of ANK3, EGR1, FBP1, FOS, KIFC3 and MAOB were associated with poor survival, while low expression of ISLR and MFAP4 were associated with worse survival (all $p < 0.05$). The final expression values for each sample and calculated results for 8 prognostic genes from GSE14359, GSE32981, and TARGET datasets were shown in the Table S3.

Differences on immune infiltration of samples in two groups

The infiltration abundance of 22 immune infiltration cells was evaluated using CIBERSORT deconvolution algorithm. Then the differences on infiltration abundance of 22 immune infiltration cells between metastatic tissue samples and primary osteosarcoma tissue samples were compared. Higher infiltration abundance of gamma delta T cells and M0 macrophages were detected in osteosarcoma tissue samples, while higher infiltration abundance of regulatory T cells (Tregs), resting dendritic cells, activated dendritic cells, activated mast cells and eosinophils were observed in metastatic osteosarcoma samples (all $p < 0.05$, Fig. 6A).

Correlation of immune infiltration with prognostic genes

The correlations of immune cells infiltration abundance with prognostic genes were evaluated using Pearson correlation analysis. Expression of these 8 prognostic genes was correlated with infiltration abundance of multiple immune cells (Fig. 6B, Table 1). For example, expression of ISLR, MFAP4, MAOB, EGR1, FOS and FBP1 showed strong positive correlations with activated dendritic cells, and expression of ANK3 and KIFC3 was positively correlated with follicular helper T cells (all $r > 0.3$, $p < 0.05$). These results indicated that these prognostic genes might be involved in immune activities in progression of osteosarcoma metastasis.

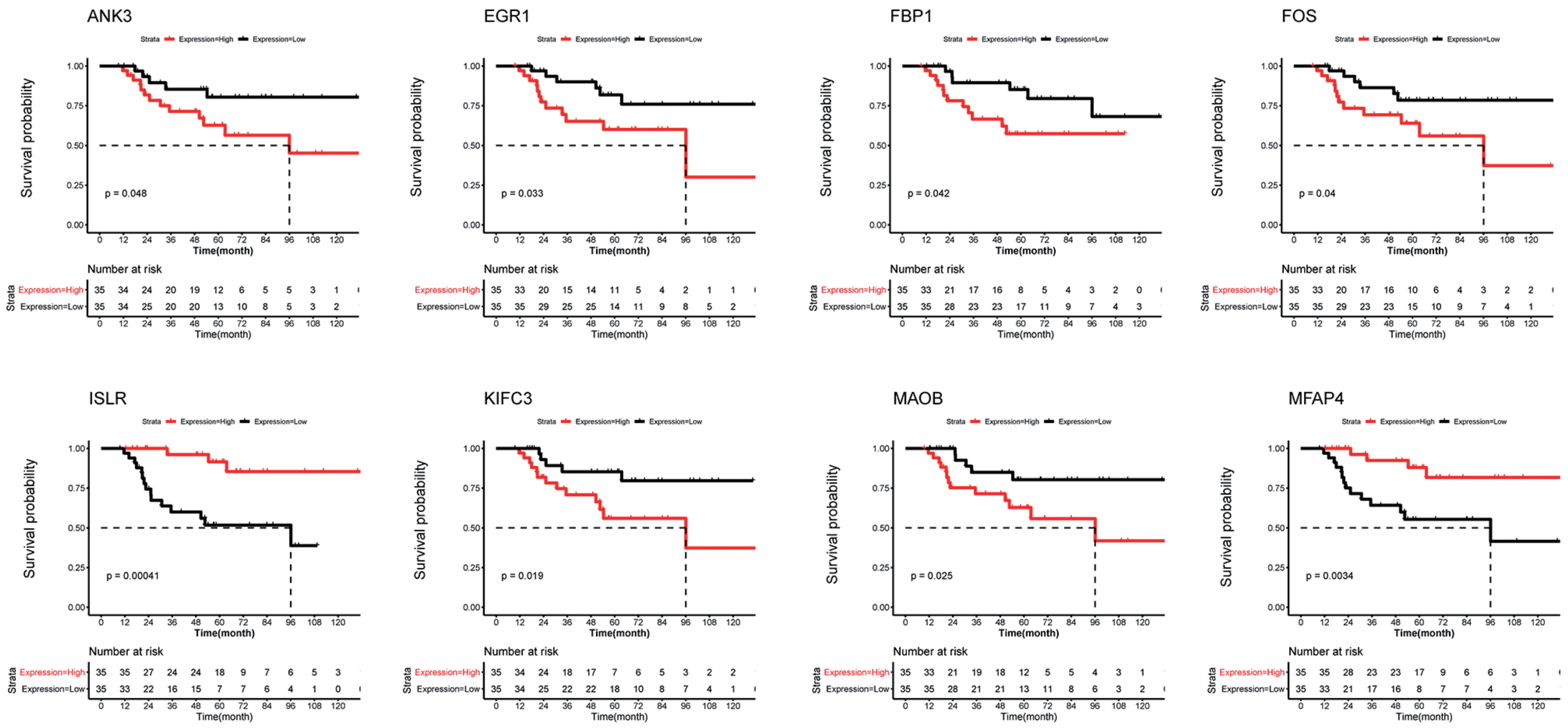

Figure 5. Survival analysis. Kaplan-Meier survival curves show the prognostic of ANK3, EGR1, FBP1, FOS, ISLR, KIFC3, MAOB and MFAP4 genes, respectively.

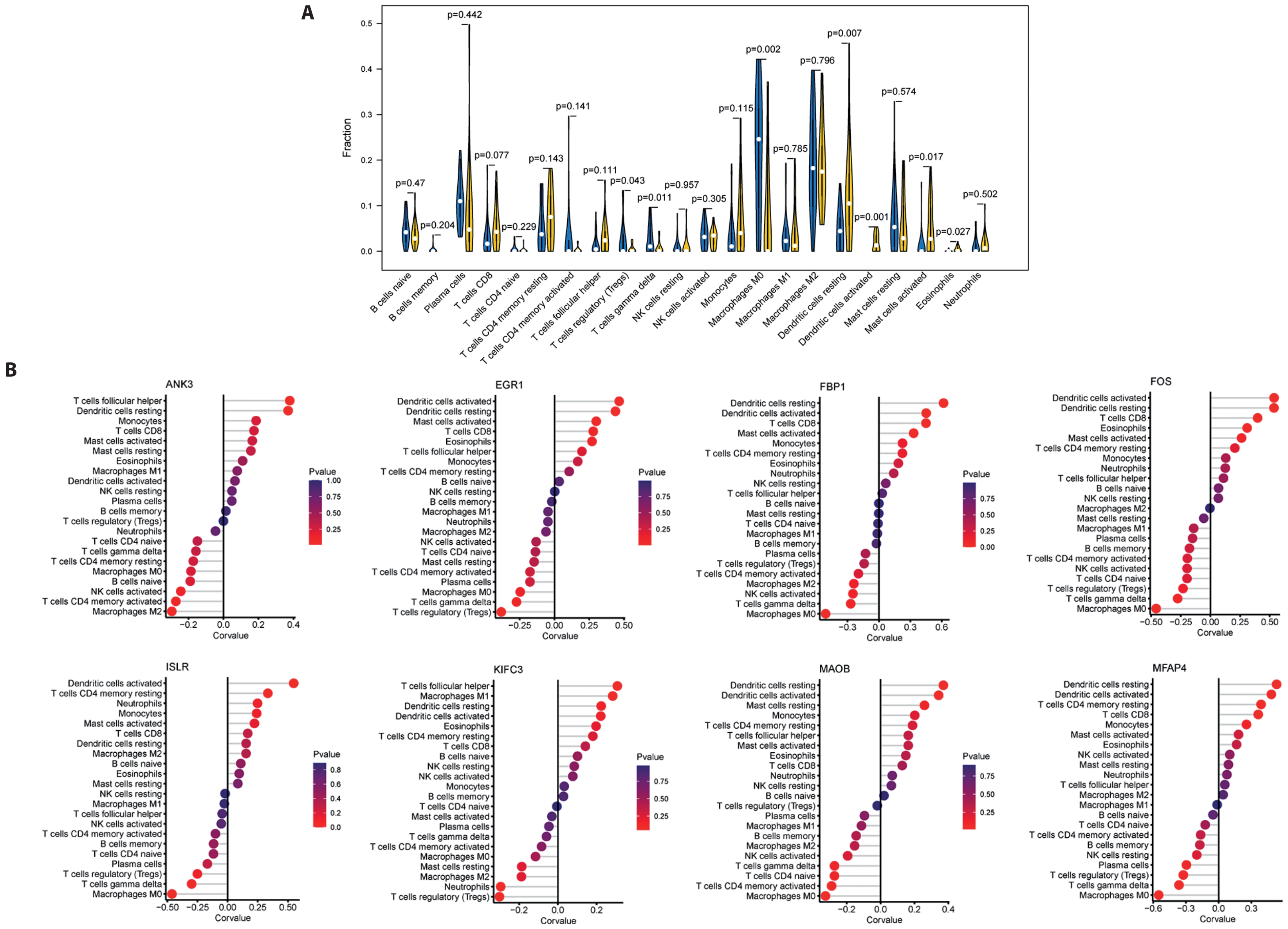

Figure 6. Correlation of immune infiltration and prognostic genes. **A.** Violin plot showed the differences on 22 immune cells infiltration in metastatic tissue samples (yellow) and primary osteosarcoma tissue samples (blue). **B.** Lollipop plots showed the correlations of prognostic genes with 22 infiltrating immune cells. x-axis represents Pearson correlation coefficient, and y-axis represents different immune cell types. Color of node from blue to red represents *p* value from insignificant to significant. (See online version for color figure.)

Transcription factors and miRNAs that targeted prognostic genes

The miRNAs that target prognostic genes were predicted. A total of 9 miRNA-target gene pairs with score > 0.9 and existed in both miRDB and miRTarBase databases were obtained, involving 10 miRNAs and 5 prognostic genes (ANK3, KIFC3, EGR1, MAOB and FOS). TRRUST online tool predicted 16 TF-target gene pairs, involving 7 TFs and 4 prognostic genes (EGR1, FBP1, MAOB and FOS). Finally, the TF-target gene pairs and miRNA-target gene pairs were integrated to construct regulatory network (Fig. 7).

Literature search by GenCLiP 3.0

GenCLiP 3.0 database was used to summarize literatures published in MEDLINE related to prognostic genes that involved in osteosarcoma (Fig. S1). Among the 8 prognostic genes, FOS (129 papers) had been widely reported in osteosarcoma, followed by EGR1 (25 papers) and FBP1 (3 papers), suggesting that these three genes played important roles in osteosarcoma. Genes, ISLR, MFAP4, MAOB, ANK3 and KIFC3 had not been reported in osteosarcoma, while they showed significant impact on prognosis of osteosarcoma patients, and their expression showed correlations with various infiltrating immune cells. Therefore, these genes might be novel targets in osteosarcoma.

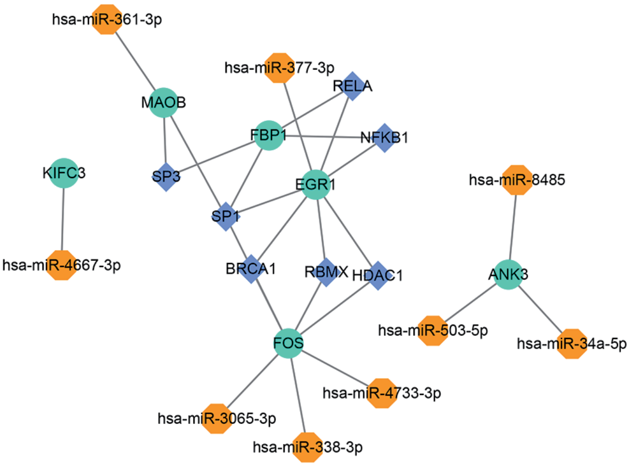

Figure 7. Transcription factors and miRNAs that targeted prognostic genes. Turquoise node represents prognostic genes; orange sexangle represent miRNAs; purple diamond represents transcription factors. (See online version for color figure.)

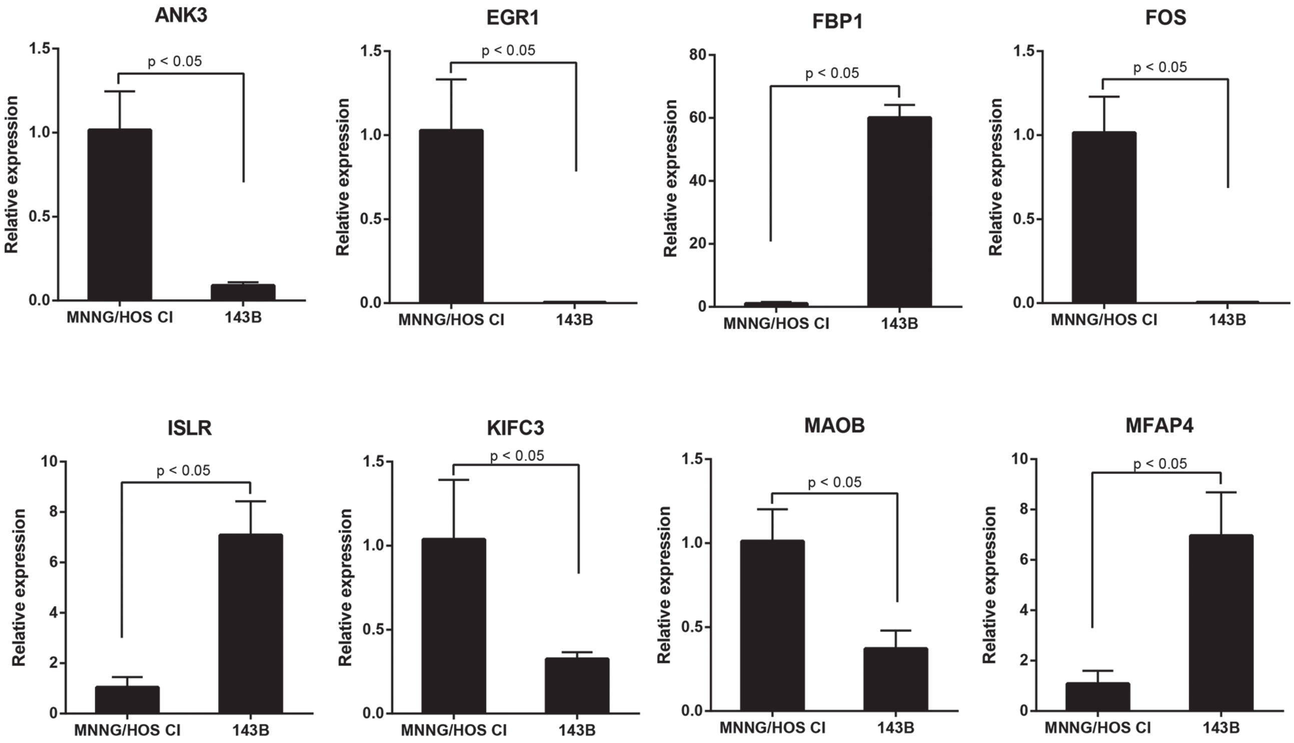

Figure 8. Expression of the prognostic genes determined by RT-qPCR. Column chart showing the expression of prognostic genes in high aggressive 143B and low aggressive MNNG/HOS Cl osteosarcoma cells.

Expression of the prognostic genes determined by RT-qPCR

Expression of the eight prognostic genes in high aggressive 143B and low aggressive MNNG/HOS Cl osteosarcoma cells were further investigated using RT-qPCR. As shown in Figure 8 and Table S4, all of these eight genes were differentially expressed between 143B and MNNG/HOS Cl cells ($p < 0.05$).

ANK3, EGR1, FOS, KIFC3, and MAOB were down-regulated in high aggressive 143B cells in comparison of relative expression in low aggressive MNNG/HOS Cl osteosarcoma cells. On the contrary FBP1, ISLR and MFAP4 were up-regulated in 143Bcells. The results suggested that these genes might be involved in aggressive progression in osteosarcoma.

Discussion

Osteosarcoma is a highly malignant tumor with high propensity for local invasion and metastasis (Ritter et al. 2010). For patients with metastasis, the treatment effect is still not ideal at present, and pulmonary metastasis is the main cause of death in patients with osteosarcoma (Eaton et al. 2021). Osteosarcoma metastasis is a complex pathological process involving a variety of signal transduction pathways (Yao et al. 2018; Zhao et al. 2018; Li et al. 2020). Therefore, in-depth study of the molecular mechanism of osteosarcoma invasion and metastasis, and seeking novel treatment targets and intervention strategies are essential to improve the efficacy for patients with osteosarcoma metastasis.

In this study, we screened 437 DEGs between primary and metastatic osteosarcoma. Genes highly co-expressed and closely related to osteosarcoma metastasis were further screened using WGCNA, which is designed to identify co-expressed gene modules and explore the associations between gene networks and the phenotypes of concern (Langfelder et al. 2008; Niemira et al. 2019). The turquoise module had the highest correlation with osteosarcoma metastasis, and contained 496 genes. After VENN analysis, 122 genes were screened, and they were enriched in chemokine activity and chemokine receptor binding. Chemokines, low molecular chemotactic cytokines, also known as small pro-inflammatory chemoattractant cytokines implicated in mediating connection within disparate cell types, and various biological processes, such as cell adhesion and migration (Cecchinato et al. 2018; Tiberio et al. 2018). Chemokines and their receptors are the most vital mechanism operating in metastasis, and organ-specific metastasis develops when tumor cells are affected by a chemokine gradient at a distance (Zlotnik et al. 2011). Increasing studies have demonstrated the involvement of chemokines and their receptors in osteosarcoma metastasis (Sun et al. 2017; Liu et al. 2019; Chao et al. 2020). For example, CXCL1/CXCR2 axis (Chao et al. 2020) and CXCL6/CXCR1/2 axis (Liu et al. 2019) have been reported to promote lung metastasis in osteosarcoma. These finding confirmed that the 122 genes are important genes involving in osteosarcoma metastasis.

Among the 122 genes, 8 genes significantly associated with prognosis were identified, including ISLR, MFAP4, MAOB, EGR1, FBP1, FOS, ANK3 and KIFC3. After literature search by GenCLiP 3.0, only three genes (EGR1, FBP1 and FOS) have been reported in osteosarcoma. For example, up-regulation of EGR1 was involved in the inhibition of osteosarcoma cell invasion by chemotherapy (Matsunoshita et al. 2011). The involvement of FBP1 in inducing programmed cell death (Xiong et al. 2020) and metabolism of osteosarcoma (Kang et al. 2018) have been reported. FOS was one of the osteosarcoma driver mutation genes (Czarnecka AM 2020). As a transcription factor belongs to AP-1 family, its activation could promote lung metastasis of osteosarcoma by inducing downstream pathways (Weekes et al. 2016). The other five genes had not been reported in osteosarcoma. However, these five genes were significantly deregulated in osteosarcoma, and their expression was associated with overall survival of patients, indicating that these genes might be potential prognostic biomarkers in metastatic osteosarcoma.

Dendritic cells (DCs) are the most important and powerful professional antigen-presenting cells in the body (Worbs et al. 2017). They are the only antigen-presenting cells that can activate naive T cells, which can effectively trigger and induce cytotoxic T cell immune response (Collin et al. 2018). DCs are involved in antigen uptake, processing and presentation. Anti-tumor therapy with DC vaccines had been reported to be safe and feasible in osteosarcoma (Himoudi et al. 2012), and showed a potent anti-tumor response (Yu et al. 2004; Zhou et al. 2020), suggesting the important role of DCs in anti-tumor response in osteosarcoma. Notably, the infiltration abundance of activated DCs showed significant differences between primary and metastatic osteosarcoma samples. Moreover, the expression of ISLR, MFAP4, MAOB, EGR1, FOS and FBP1 were all showed strong positive correlations with activated DCs, and ANK3 with resting DCs. Except for DCs, the 8 prognostic genes also showed correlations with various tumor-infiltrating immune cells, such as macrophages, T cells regulatory (Tregs), CD8 T cells. The above findings suggested the importance of these prognostic genes in anti-tumor response in osteosarcoma.

Considering the importance of these prognostic genes in osteosarcoma, we predicted TFs and miRNAs that could target these genes to further investigate their potential molecular regulation mechanism. For example, ANK3 was regulated by miR-8485, miR-503-5p and miR-34a-5p. The role of miR-503 in regulating osteosarcoma cell invasion and metastasis had been reported in many studies, and had been considered as target for the treatment of osteosarcoma (Guo et al. 2016; Li et al. 2017a; Lv et al. 2018). Various studies had reported the involvement of miR-34a in inhibiting invasion and metastasis in osteosarcoma, and in mediating chemotherapy sensitivity in osteosarcoma (Zhao et al. 2013; Li et al. 2017b; Wen et al. 2017). However, the associations of these miRNAs with ANK3 have not been investigated in osteosarcoma. Our study provided several targets to investigate their potential molecular regulation mechanism.

In conclusion, we identified eight osteosarcoma metastasis-related genes. Their expression was associated with prognosis, and showed strong correlations with various tumor-infiltrating immune cells in osteosarcoma. These genes might be potential prognostic genes in osteosarcoma and targets for investigation the molecular regulation mechanism.

Conflict of interest. All authors declare no conflicts of interest in this paper.

References

Cecchinato V, Uguccioni M (2018): Insight on the regulation of chemokine activities. J. Leukoc. Biol. **104,** 295-300
https://doi.org/10.1002/JLB.3MR0118-014R

Chao CC, Lee CW, Chang TM, Chen PC, Liu JF (2020): CXCL1/CXCR2 paracrine axis contributes to lung metastasis in osteosarcoma. Cancers **12,** 459
https://doi.org/10.3390/cancers12020459

Chen C, Xie L, Ren T, Huang Y, Xu J, Guo W (2021): Immunotherapy for osteosarcoma: Fundamental mechanism, rationale, and recent breakthroughs. Cancer Lett. **500,** 1-10
https://doi.org/10.1016/j.canlet.2020.12.024

Chen Y, Zhao B, Wang X (2020): Tumor infiltrating immune cells (TIICs) as a biomarker for prognosis benefits in patients with osteosarcoma. BMC Cancer **20,** 1022
https://doi.org/10.1186/s12885-020-07536-3

Collin M, Bigley V (2018): Human dendritic cell subsets: an update. Immunology **154,** 3-20
https://doi.org/10.1111/imm.12888

Czarnecka AMSK, Firlej W, Bartnik E, Sobczuk P, Fiedorowicz M, Grieb P, Rutkowski P (2020): Molecular biology of osteosarcoma. Cancers (Basel) **12,** 2130
https://doi.org/10.3390/cancers12082130

Eaton B.R, Schwarz R, Vatner R, Yeh B, Claude L, Indelicato DJ, Laack N (2021): Osteosarcoma. Pediatr. Blood Cancer **68,** e28352
https://doi.org/10.1002/pbc.28355

Farhood B, Najafi M, Mortezaee K (2019): CD8(+) cytotoxic T lymphocytes in cancer immunotherapy: A review. J. Cell. Physiol. **234,** 8509-8521
https://doi.org/10.1002/jcp.27782

Garaud S, Buisseret L, Solinas C, Gu-Trantien C, de Wind A, Van den Eynden G, Naveaux C, Lodewyckx JN, Boisson A, Duvillier H (2019): Tumor infiltrating B-cells signal functional humoral immune responses in breast cancer. JCI Insight **5,** e129641
https://doi.org/10.1172/jci.insight.129641

Gianferante DM, Mirabello L, Savage SA (2017): Germline and somatic genetics of osteosarcoma – connecting aetiology, biology and therapy. Nat. Rev. Endocrinol. **13,** 480-491
https://doi.org/10.1038/nrendo.2017.16

Guo X, Zhang J, Pang J, He S, Li G, Chong Y, Li C, Jiao Z, Zhang S, Shao M (2016): MicroRNA-503 represses epithelial-mesenchymal transition and inhibits metastasis of osteosarcoma by targeting c-myb. Tumour Biol. **37,** 9181-9187
https://doi.org/10.1007/s13277-016-4797-4

Harrison DJ, Geller DS, Gill JD, Lewis VO, Gorlick R (2018): Current and future therapeutic approaches for osteosarcoma. Expert Rev. Anticancer Ther. **18,** 39-50
https://doi.org/10.1080/14737140.2018.1413939

Heymann MF, Lézot F, Heymann D (2019): The contribution of immune infiltrates and the local microenvironment in the pathogenesis of osteosarcoma. Cell. Immunol. **343,** 103711
https://doi.org/10.1016/j.cellimm.2017.10.011

Himoudi N, Wallace R, Parsley KL, Gilmour K, Barrie AU, Howe K, Dong R, Sebire NJ, Michalski A, Thrasher AJ, Anderson J (2012): Lack of T-cell responses following autologous tumour lysate pulsed dendritic cell vaccination, in patients with relapsed osteosarcoma. Clin. Transl. Oncol. **14,** 271-279
https://doi.org/10.1007/s12094-012-0795-1

Kang Y, Zhu X, Xu Y, Tang Q, Huang Z, Zhao Z, Lu J, Song G, Xu H, Deng C, Wang J (2018): Energy stress-induced lncRNA HAND2-AS1 represses HIF1α-mediated energy metabolism and inhibits osteosarcoma progression. Am. J. Cancer Res. **8,** 526-537

Langfelder P, Horvath S (2008): WGCNA: an R package for weighted correlation network analysis. BMC Bioinformatics **9,** 559
https://doi.org/10.1186/1471-2105-9-559

Li J, Wu QM, Wang XQ, Zhang CQ (2017): Long noncoding RNA miR210HG sponges miR-503 to facilitate osteosarcoma cell invasion and metastasis. DNA Cell Biol. **36,** 1117-1125
https://doi.org/10.1089/dna.2017.3888

Li QC, Xu H, Wang X, Wang T, Wu J (2017): miR-34a increases cisplatin sensitivity of osteosarcoma cells in vitro through upregulation of c-Myc and Bim signal. Cancer Biomark. **21,** 135-144
https://doi.org/10.3233/CBM-170452

Li X, Huang Q, Wang S, Huang Z, Yu F, Lin J (2020): HER4 promotes the growth and metastasis of osteosarcoma via the PI3K/AKT pathway. Acta Biochim. Biophys. Sin. **52,** 345-362
https://doi.org/10.1093/abbs/gmaa004

Lilienthal I, Herold N (2020): Targeting molecular mechanisms underlying treatment efficacy and resistance in osteosarcoma: A review of current and future strategies. Int. J. Mol. Sci. **21,** 6885
https://doi.org/10.3390/ijms21186885

Liu G, An L, Zhang H, Du P, Sheng Y (2019): Activation of CXCL6/CXCR1/2 axis promotes the growth and metastasis of osteosarcoma cells in vitro and in vivo. Front. Pharmacol. **10,** 307
https://doi.org/10.3389/fphar.2019.00307

Liu Y, Feng W, Dai Y, Bao M, Yuan Z, He M, Qin Z, Liao S, He J, Huang Q, Yu Z, Zeng Y, Guo B (2021): Single-cell transcriptomics reveals the complexity of the tumor microenvironment of treatment-naive osteosarcoma. Front. Oncol. **11,** 709210 https://doi.org/10.3389/fonc.2021.709210

Luo ZW, Liu PP, Wang ZX, Chen CY, Xie H (2020): Macrophages in Osteosarcoma Immune Microenvironment: Implications for Immunotherapy. Front. Oncol. **10,** 586580 https://doi.org/10.3389/fonc.2020.586580

Lv T, Liu Y, Li Z, Huang R, Zhang Z, Li J. (2018): miR-503 is downregulated in osteosarcoma and suppressed MG63 proliferation and invasion by targeting VEGFA/Rictor. Cancer Biomark **23,** 315-322 https://doi.org/10.3233/CBM-170906

Matsunoshita Y, Ijiri K, Ishidou Y, Nagano S, Yamamoto T, Nagao H, Komiya S, Setoguchi T (2011): Suppression of osteosarcoma cell invasion by chemotherapy is mediated by urokinase plasminogen activator activity via up-regulation of EGR1. PLoS One **6,** e16234 https://doi.org/10.1371/journal.pone.0016234

Moore C, Eslin D, Levy A, Roberson J, Giusti V, Sutphin R (2010): Prognostic significance of early lymphocyte recovery in pediatric osteosarcoma. Pediatr. Blood Cancer **55,** 1096-1102 https://doi.org/10.1002/pbc.22673

Niemira M, Collin F, Szalkowska A, Bielska A, Chwialkowska K, Reszec J, Niklinski J, Kwasniewski M, Kretowski A (2019): Molecular signature of subtypes of non-small-cell lung cancer by large-scale transcriptional profiling: Identification of key modules and genes by Weighted Gene Co-Expression Network Analysis (WGCNA). Cancers (Basel) **12,** 37 https://doi.org/10.3390/cancers12010037

Ritter J, Bielack SS (2010): Osteosarcoma. Ann. Oncol. **21,** vii320-325 https://doi.org/10.1093/annonc/mdq276

Sayles LC, Breese MR, Koehne AL, Leung SG, Lee AG, Liu HY, Spillinger A, Shah AT, Tanasa B, Straessler K (2019): Genome-informed targeted therapy for osteosarcoma. Cancer Discov. **9,** 46-63 https://doi.org/10.1158/2159-8290.CD-17-1152

Sun K, Gong C, Peng H, Fang H, Zhou J, Li J, Chen S, Zheng H (2017): High CCL5 expression is associated with osteosarcoma metastasis and poor prognosis of patients with osteosarcoma. Mol. Med. Rep. **16,** 6953-6957 https://doi.org/10.3892/mmr.2017.7458

Tas F, Erturk K (2017): Tumor infiltrating lymphocytes (TILs) may be only an independent predictor of nodal involvement but not for recurrence and survival in cutaneous melanoma patients. Cancer Invest. **35,** 501-505 https://doi.org/10.1080/07357907.2017.1351984

Tiberio L, Del Prete A, Schioppa T, e Sozio F, Bosisio D, Sozzani S (2018): Chemokine and chemotactic signals in dendritic cell migration. Cell. Mol. Immunol. **15,** 346-352 https://doi.org/10.1038/s41423-018-0005-3

Wang SS, Liu W, Ly D (2019): Tumor-infiltrating B cells: their role and application in anti-tumor immunity in lung cancer. Cell. Mol. Immunol. **16,** 6-18 https://doi.org/10.1038/s41423-018-0027-x

Weekes D, Kashima TG, Zandueta C, Perurena N, Thomas DP, Sunters A, Vuillier C, Bozec A, El-Emir E, Miletich I (2016): Regulation of osteosarcoma cell lung metastasis by the c-Fos/AP-1 target FGFR1. Oncogene **35,** 2852-2861 https://doi.org/10.1038/onc.2015.344

Wen J, Zhao YK, Liu Y, Liu Y, Zhao JF (2017): MicroRNA-34a inhibits tumor invasion and metastasis in osteosarcoma partly by effecting C-IAP2 and Bcl-2. Tumour Biol. **39,** 1010428317705761 https://doi.org/10.1177/1010428317705761

Worbs T, Hammerschmidt SI, Förster R (2017): Dendritic cell migration in health and disease. Nat. Rev. Immunol. **17,** 30-48 https://doi.org/10.1038/nri.2016.116

Xiong X, Zhang J, Li A, Dai L, Qin S, Wang P, Liu W, Zhang Z, Li X, Liu Z (2020): GSK343 induces programmed cell death through the inhibition of EZH2 and FBP1 in osteosarcoma cells. Cancer Biol. Ther. **21,** 213-222 https://doi.org/10.1080/15384047.2019.1680061

Yao Z, Han L, Chen Y, He F, Sun B, Kamar S, Zhang Y, Yang Y, Wang C, Yang Z (2018): Hedgehog signalling in the tumourigenesis and metastasis of osteosarcoma, and its potential value in the clinical therapy of osteosarcoma. Cell Death Dis. **9,** 701 https://doi.org/10.1038/s41419-018-0647-1

Yu Z, Fan Q, Hao X, Long H (2004): Specific antitumor effects of tumor vaccine produced by electrofusion between osteosarcoma cell and dendritic cell in rats. Cell. Mol. Immunol. **1,** 454-460 https://doi.org/10.4993/acrt.13.43

Zhao H, Ma B, Wang Y, Han T, Zheng L, Sun C, Liu T, Zhang Y, Qiu X, Fan Q (2013): miR-34a inhibits the metastasis of osteosarcoma cells by repressing the expression of CD44. Oncol. Rep. **29,** 1027-1036 https://doi.org/10.3892/or.2013.2234

Zhao Z, Jia Q, Wu MS, Xie X, Wang Y, Song G, Zou CY, Tang Q, Lu J, Huang G, Wang J, Lin DC, Koeffler HP, et al. (2018): Degalactotigonin, a natural compound from Solanum nigrum L, inhibits growth and metastasis of osteosarcoma through GSK3β inactivation-mediated repression of the Hedgehog/Gli1 pathway. Clin. Cancer Res. **24,** 130-144 https://doi.org/10.1158/1078-0432.CCR-17-0692

Zhou Y, Slone N, Chrisikos TT, Kyrysyuk O, Babcock RL, Medik YB, Li HS, Kleinerman ES, Watowich SS (2020): Vaccine efficacy against primary and metastatic cancer with in vitro-generated CD103(+) conventional dendritic cells. J. Immunother. Cancer **8,** e000474 https://doi.org/10.1136/jitc-2019-000474

Zitvogel L, Apetoh L, Ghiringhelli F, Kroemer G (2008): Immunological aspects of cancer chemotherapy. Nat. Rev. Immunol. **8,** 59-73 https://doi.org/10.1038/nri2216

Zlotnik A, Burkhardt AM, Homey B (2011): Homeostatic chemokine receptors and organ-specific metastasis. Nat. Rev. Immunol. **11,** 597-606 https://doi.org/10.1038/nri3049

Received: June 10, 2022
Final version accepted: September 13, 2022

doi: 10.4149/gpb_2022050

Supplementary Material

Immune-based prognostic biomarkers associated with metastasis of osteosarcoma

Teng Ma, Changliang Peng, Dongjin Wu, Song Yang, Li Ji, Zhang Cheng and Chunzheng Gao

Department of Spine Surgery, The Second Hospital of Shandong University, Shandong University, Jinan, China

Supplementary Tables

Table S1. The primers sequences in RT-qPCR

Primers	Sequence (5'–3')
ANK3-F	ACCGCAGAGTGAAGATGCAA
ANK3-R	AAGCCCATGTAACCCTCTGC
EGR1-F	CACCTGACCGCAGAGTCTTT
EGR1-R	CTGACCAAGCTGAAGAGGGG
FBP1-F	ACCCCGCTAACAAGAAGAGC
FBP1-R	CTTCAGGAACTCGAGCACGT
FOS-F	CAAGCGGAGACAGACCAACT
FOS-R	GTGAGCTGCCAGGATGAACT
LSLR-F	ACCTCAGTGCCCTCCAATTG
LSLR-R	CGGTTGTGGTTGAGTTGCAG
KIFC3-F	TGAAGGCTGTGCACGAGAAT
KIFC3-R	GTTGCTGTTGACCTCCTCGA
MAOB-F	TGCATGCCATGGGGAAGATT
MAOB-R	CACGGAGGGCAAATGTCTCT
MFAP4-F	GGGACCAGGACCTCTTTGTG
MFAP4-R	CTCAGTGCGTTTGAGGGAGT
βactin-F	AGACCTGTACGCCAACACAG
βactin-R	CGGACTCGTCATACTCCTGC

Table S2. The differentially expressed genes

	logFC	AveExpr	t	*p* value	adj.*p* Val.	B
SFTPC	7.370569367	10.90657768	9.865120342	1.49E-12	9.41E-09	18.06263968
SFTPD	5.995352661	10.45078239	9.358640404	6.99E-12	1.75E-08	16.63940072
CYP4B1	5.093371688	9.664530522	7.509479985	2.55E-09	2.70E-06	11.15327623
SFTPB	4.6761002	10.48662666	9.303729219	8.28E-12	1.75E-08	16.48287382
SCGB1A1	4.564632899	10.30086232	7.985784875	5.41E-10	8.57E-07	12.60505479
C4BPA	3.812689397	10.28622131	7.195905202	7.17E-09	6.49E-06	10.18605716
CXCL2	3.688456527	11.84087642	7.53506117	2.35E-09	2.70E-06	11.23181035
LAMP3	3.563030445	10.47946081	6.161984418	2.22E-07	7.83E-05	6.956117908

(continued)

Table S2. (continued)

	logFC	AveExpr	t	*p* value	adj.*p* Val.	B
MARCO	3.43551937	9.90625359	6.340243809	1.23E-07	5.19E-05	7.515437418
C7	3.225358638	10.45573899	5.266239766	4.34E-06	0.000640238	4.157587402
TACSTD2	3.01858119	10.31660006	6.383550377	1.06E-07	4.99E-05	7.651266619
FOSB	2.945925754	11.26159381	6.275010752	1.53E-07	6.05E-05	7.310786403
ABCA3	2.927563479	10.05923667	5.520438882	1.88E-06	0.000396579	4.947375261
FOXF1	2.880404773	11.14963673	6.518825304	6.78E-08	3.90E-05	8.075297655
CCL18	2.864239847	11.46137854	5.224602036	4.98E-06	0.00071748	4.028779785
CXCL3	2.790427599	9.643083168	4.951166211	1.22E-05	0.001378716	3.187892689
CLDN18	2.778427203	9.479185627	5.026935815	9.51E-06	0.001230902	3.419953045
SLC34A2	2.725166429	10.17538898	6.434991931	8.96E-08	4.73E-05	7.812565347
CEACAM6	2.591220244	10.40734869	4.724366366	2.54E-05	0.002252694	2.498459032
KRT19	2.589559704	9.58553095	3.859664313	0.000380764	0.01388348	-0.028937956
TREM1	2.551922789	10.0716635	5.175084606	5.86E-06	0.000825383	3.87583476
C3	2.532963219	12.73651915	4.145540118	0.000158595	0.008545486	0.785053292
MFAP4	2.497812562	11.18533685	4.231041881	0.000121542	0.00726842	1.033124087
FOS	2.483668532	15.58785497	6.230861802	1.77E-07	6.59E-05	7.172257246
SERPINA1	2.461364969	13.84798856	5.432232934	2.51E-06	0.000482632	4.672721731
CES1	2.447798098	10.08636948	5.290122137	4.01E-06	0.00061498	4.231547031
GATA6	2.443546603	10.23767627	5.698015233	1.04E-06	0.000253983	5.501833239
PGC	2.33013864	11.77952334	5.403029567	2.77E-06	0.000501128	4.581919933
SPINT2	2.297845552	11.4219261	7.017713274	1.29E-08	1.02E-05	9.633075127
ANXA3	2.284352233	10.53045658	4.123977835	0.000169554	0.008882692	0.722809897
EDN1	2.281944958	9.815778576	5.011464133	1.00E-05	0.001233331	3.372503826
MMP7	2.239351296	10.40266076	3.885943865	0.000351646	0.013602304	0.044822266
CLIC3	2.183524617	10.63777841	4.340056573	8.64E-05	0.005720479	1.352180338
HPGD	2.131237211	11.06965753	4.463979087	5.84E-05	0.004404957	1.718358396
FCN3	2.110150092	10.55059028	4.554896851	4.37E-05	0.003552008	1.989189046
HP	2.105975218	9.325646644	3.706242958	0.000603304	0.017954679	-0.454842292
LTF	2.059369097	9.526203581	4.173224662	0.000145531	0.008236799	0.865158986
CD69	2.026097736	10.40499555	5.000046971	1.04E-05	0.001242333	3.33750986
EPS8L2	2.011283774	11.13054964	5.344024647	3.36E-06	0.000546379	4.398674082
TYRP1	1.987540029	9.670007598	4.994198685	1.06E-05	0.001242798	3.319591559
VIPR1	1.985521937	9.983720904	4.315371193	9.33E-05	0.00591603	1.279672093
SLC6A14	1.966391525	9.429590919	3.369761852	0.001610288	0.032508328	-1.357840478
CNTN6	1.962915051	9.709770935	3.741951943	0.000542376	0.017524386	-0.356451318
EGR2	1.958271665	11.49991324	5.820223811	6.94E-07	0.000191294	5.884324997
ZFP36	1.908730965	14.82154492	5.37885931	3.00E-06	0.000513843	4.50682056
MOXD1	1.895269358	10.2577731	4.94395331	1.25E-05	0.001386692	3.165843662
CCL21	1.869350841	10.88235609	4.444737325	6.20E-05	0.004627052	1.661270038
INHBA	1.860318021	12.63943148	4.655444279	3.17E-05	0.002677721	2.290680682
NR4A2	1.833285993	11.97464556	4.757613375	2.28E-05	0.002125913	2.598994207
LYZ	1.793229647	13.63892444	4.220116274	0.000125758	0.007381284	1.001315787
SLPI	1.789318721	12.62353779	3.807958797	0.000445013	0.015585296	-0.173387257
DMBT1	1.772006246	9.698637054	3.782567829	0.000480282	0.016280801	-0.243987189
CDH1	1.762165236	12.42689898	3.487285987	0.001148107	0.027305836	-1.047634183
JUNB	1.756404472	12.54151415	6.61304083	4.95E-08	3.38E-05	8.370319683
EGR1	1.745012312	14.36706334	6.590499255	5.34E-08	3.38E-05	8.299761149
FBP1	1.73847279	10.95046109	4.164520092	0.000149521	0.008277755	0.839949438

(continued)

Table S2. (continued)

	logFC	AveExpr	t	*p v*alue	adj.*p* Val.	B
SPINT1	1.719542508	9.82246064	5.088829494	7.77E-06	0.00104831	3.610083673
ABCC3	1.719470547	10.3661535	5.31313457	3.72E-06	0.000589803	4.302864851
DUSP1	1.697979607	15.34110942	5.792961772	7.60E-07	0.000197358	5.798948083
RARRES2	1.681545146	12.12480741	3.177333125	0.002769626	0.044223322	-1.852601878
SPOCK2	1.660063245	11.81087442	3.735564765	0.00055282	0.017524386	-0.374083971
MEST	1.647952884	13.78445181	3.116311467	0.003278858	0.048224316	-2.005875438
KCNK3	1.633107342	9.660781098	3.947794902	0.000291369	0.012395895	0.219310563
AQP9	1.626121272	8.812490641	3.540298207	0.000983985	0.025050124	-0.905832187
CAV2	1.62105079	13.03921957	6.3728552	1.10E-07	4.99E-05	7.617724611
CAV1	1.61655869	15.2102324	4.774155296	2.16E-05	0.002045476	2.649086697
CA4	1.610914565	9.758503508	4.231640539	0.000121315	0.00726842	1.034867899
PDLIM3	1.605478429	10.52441587	3.473382499	0.001195308	0.027754789	-1.084634944
CLDN4	1.586310546	10.19828073	4.875667605	1.56E-05	0.001591481	2.957482763
BCHE	1.579593053	10.32121077	3.133176724	0.003129914	0.046820811	-1.963694375
TMC5	1.551370173	8.729737746	4.095547799	0.000185137	0.00929555	0.640942275
NINJ2	1.516299389	10.82201159	3.47800437	0.001179415	0.027690042	-1.072343791
ISLR	1.516135301	11.35174028	4.008266723	0.000242185	0.011203013	0.39107654
TM4SF1	1.510927203	13.31082425	5.97873731	4.10E-07	0.000129815	6.381183802
IL6	1.503834985	10.35078045	3.237692905	0.002340163	0.04033898	-1.699239406
FBLN5	1.495361931	11.75332699	3.200057377	0.002599856	0.042925223	-1.795065757
MLPH	1.494618418	11.42126236	3.695459352	0.000622965	0.018104048	-0.484464056
HSD11B1	1.485689159	9.920017498	3.308741474	0.001915512	0.036157354	-1.516553381
CLDN5	1.480898561	11.33687276	3.42550315	0.001372459	0.029896962	-1.211439341
CRTAC1	1.471269353	10.0669625	3.575053098	0.000888857	0.0231871	-0.81225602
VWF	1.470135557	12.93483431	3.371634027	0.001601699	0.032438236	-1.352945083
NR4A1	1.464988505	10.87761231	5.847228003	6.34E-07	0.000182812	5.968919636
CTSH	1.438229445	15.13269779	4.357092861	8.18E-05	0.005578722	1.402307352
ATF3	1.437242537	12.39900302	4.005978948	0.00024389	0.011203013	0.384557766
TMPRSS2	1.431682453	9.501097932	3.883687542	0.000354059	0.013602304	0.038480381
NPR3	1.422268385	9.572510771	5.014652169	9.90E-06	0.001233331	3.382278408
TBC1D2	1.404232012	10.79789101	3.964452435	0.00027693	0.012106595	0.266511686
ALOX5AP	1.393413722	13.33449988	3.700330813	0.000614008	0.01795497	-0.471087778
G0S2	1.383986055	12.34954182	4.850658466	1.69E-05	0.001698497	2.88135029
CD74	1.375494689	14.96091391	3.361387492	0.001649248	0.032852907	-1.379719188
TIMP3	1.360430013	14.15017476	4.256678002	0.000112183	0.006971842	1.107882389
SCNN1A	1.358660275	10.47609728	4.716610965	2.60E-05	0.002252694	2.475035708
AQP3	1.358590017	10.93755699	5.648708405	1.23E-06	0.000288059	5.347701632
LTBP2	1.352534716	13.04933997	3.489828819	0.001139669	0.027305836	-1.040858456
MYH11	1.348560091	11.49231816	3.351501863	0.001696395	0.033395803	-1.405506716
TGM2	1.331304314	9.458121671	3.430094326	0.001354441	0.029811807	-1.199321718
ALOX5	1.329742492	11.49824558	3.694115055	0.000625459	0.018104048	-0.488153758
EMP2	1.325430976	14.96717275	5.579211914	1.54E-06	0.000337691	5.130680515
IL1B	1.325084456	11.17641441	4.375271603	7.73E-05	0.005325213	1.455872573
CITED2	1.322531227	11.20246125	4.596501821	3.83E-05	0.003191743	2.113698945
ICAM1	1.319068267	11.31862346	4.328270666	8.96E-05	0.00585665	1.317543042
ROS1	1.312634764	10.02133643	3.217191282	0.002478415	0.041562621	-1.751522332
ALCAM	1.311222198	12.74821019	4.040228978	0.000219549	0.010543334	0.482315046
MAOA	1.297126732	12.06265162	3.178204093	0.00276293	0.044223322	-1.850401184

(continued)

Table S2. (continued)

	logFC	AveExpr	t	*p* *v*alue	adj.*p* Val.	B
KIT	1.292814336	11.23566427	3.972942977	0.000269839	0.012045844	0.290604087
S100A9	1.269887021	11.46659928	3.378110315	0.001572322	0.032151448	-1.335999016
HLA-DQB1	1.261946914	12.91139763	3.623296957	0.000771322	0.020787833	-0.681579049
FOXA1	1.255386078	9.322237105	3.62281165	0.000772427	0.020787833	-0.68289805
NFKBIA	1.244109409	14.30851538	4.579976684	4.03E-05	0.003321208	2.064202811
F3	1.232219764	11.61525064	3.233237857	0.002369569	0.04059648	-1.710617277
RASGRP1	1.228752193	10.13895374	3.569955562	0.000902236	0.023343964	-0.826010755
MAP3K8	1.227221119	10.35627788	3.169025029	0.002834272	0.044435026	-1.873575872
FBLN1	1.225714403	11.75066583	3.197836314	0.002616005	0.042960758	-1.800700134
NEBL	1.222716311	9.473400531	3.702416654	0.000610211	0.01795497	-0.465357727
CEBPA	1.216693769	11.48119423	3.125383554	0.003197927	0.047363694	-1.983202893
BCL2A1	1.214249472	11.08908792	4.234272622	0.000120322	0.00726842	1.042535924
SORL1	1.189106115	10.48388949	3.509335069	0.00107689	0.02656188	-0.988793496
TNFSF10	1.186110657	12.55470097	3.484862308	0.001156205	0.027347693	-1.054089942
CSTA	1.186013486	10.6806727	3.400367038	0.001475231	0.030965196	-1.277622989
IER3	1.174925249	14.10707861	3.575287659	0.000888246	0.0231871	-0.811622857
LCP2	1.172098329	11.18126264	4.093136231	0.000186521	0.00929555	0.634008511
CNN1	1.168875911	10.13529493	3.407965896	0.001443412	0.030917989	-1.257643544
ACTA2	1.163374585	15.04248754	3.727229353	0.000566741	0.017610649	-0.397072986
KRT18	1.146907349	12.85172823	3.903972707	0.000332929	0.013357198	0.09555602
PLAC8	1.14421453	12.14308389	3.454744038	0.001261502	0.028356958	-1.134111247
AQP1	1.13917439	12.84088411	5.008118323	1.01E-05	0.001233331	3.362246982
JUP	1.136303417	11.46169766	4.032986297	0.000224491	0.010619755	0.461613406
MAOB	1.133608705	10.96669401	3.158801514	0.002915779	0.04459359	-1.89933992
FOXF2	1.114333383	10.54383984	3.586685672	0.000859037	0.02259516	-0.78082966
LBH	1.112882345	14.76009411	4.09109632	0.0001877	0.00929555	0.628144648
PLSCR4	1.10084641	12.45414102	3.409068069	0.001438852	0.030917989	-1.254743582
AMIGO2	1.100144396	12.49568104	3.712266162	0.000592584	0.01788758	-0.438278538
MYH9	1.099991109	12.1842842	5.785755148	7.78E-07	0.000197358	5.776383541
CXCL1	1.09709642	10.41595472	3.940044431	0.000298334	0.012524094	0.19737849
ELN	1.09461623	11.21322348	3.394466946	0.001500397	0.031264263	-1.29311884
KRT8	1.082892807	10.73335779	3.925908326	0.000311455	0.012737497	0.157425687
EPHX1	1.081228723	11.53870042	4.908551874	1.40E-05	0.00147803	3.057735663
ARHGEF16	1.052286675	9.71719617	3.305518165	0.001933077	0.036181705	-1.524891098
ABLIM3	1.03633766	11.77705826	3.19172036	0.002660964	0.043473838	-1.816202969
JUN	1.03407635	14.8488392	3.770464404	0.00049803	0.016615855	-0.277561995
EDNRB	1.00344245	10.98172304	3.184368573	0.002715975	0.043878408	-1.834814906
TACC1	1.002858157	13.16328083	4.930874166	1.30E-05	0.001422003	3.12588143
CCL19	0.997569905	10.1751892	3.240914513	0.002319114	0.04033898	-1.691005907
EPAS1	0.988333717	12.04607059	3.532962462	0.001005275	0.025415514	-0.925522084
PERP	0.977035941	10.84217381	3.788456351	0.00047187	0.016218013	-0.227633981
ARRB1	0.974627177	10.38835671	3.998410042	0.000249612	0.011383382	0.363002336
PTPRF	0.97376641	12.22378806	3.243502477	0.002302336	0.04033898	-1.68438833
TNFAIP3	0.970405379	12.21020243	3.678115688	0.000655888	0.018728251	-0.532016294
MST1R	0.955682216	9.331715999	3.172920666	0.002803784	0.044354488	-1.863745357
SDC4	0.952790602	13.39800901	4.305768144	9.62E-05	0.006036815	1.251505634
DUSP6	0.94617424	13.50764432	3.362355776	0.001644698	0.032852907	-1.377191032
F11R	0.943706139	11.41765617	3.822250143	0.000426276	0.015180707	-0.133552323

(continued)

Table S2. (continued)

	logFC	AveExpr	t	*p v*alue	adj.*p* Val.	B
CEBPD	0.938347936	14.98385351	3.522816394	0.00103545	0.026034736	-0.952719635
SOCS3	0.931813325	10.1921891	3.222819291	0.002439711	0.041240873	-1.737189426
ITPR3	0.929371472	11.28367989	3.327118842	0.001818231	0.035139524	-1.468927839
ANK3	0.928508677	9.81622411	3.372571875	0.001597412	0.032438236	-1.35049221
RUNX3	0.927276387	12.04512587	3.318713848	0.001862125	0.035769723	-1.490728382
CD44	0.926764284	13.87856834	3.739167298	0.000546906	0.017524386	-0.364140493
PPP1R15A	0.921738161	12.15637866	4.783852223	2.10E-05	0.002012452	2.6784728
SLCO3A1	0.919385375	11.03749044	3.269415413	0.002140562	0.038879722	-1.617956952
NEDD9	0.904335028	12.37411436	3.108251975	0.003352372	0.049002403	-2.025983413
KIFC3	0.901054965	12.0293576	3.107972109	0.003354952	0.049002403	-2.026681088
CTDSPL	0.900562674	11.37042805	3.598831758	0.000828926	0.021893998	-0.747959803
IER2	0.898382592	14.5702808	4.152153593	0.000155374	0.008490653	0.804170269
VAMP2	0.894947731	10.93821092	3.699982874	0.000614644	0.01795497	-0.472043452
MAP3K5	0.888941238	11.96328344	3.951523943	0.000288074	0.01233854	0.229869666
ALDH2	0.886362284	15.54811848	3.165374721	0.002863124	0.044435026	-1.882780701
EGR3	0.885384358	10.91910124	3.449186406	0.001281909	0.028612744	-1.14883614
RBPMS	0.882586865	10.70951226	4.091538657	0.000187444	0.00929555	0.629416073
RHOBTB2	0.85235382	9.050588405	3.473843824	0.001193713	0.027754789	-1.083408517
TRIB2	0.84679748	12.67364071	3.319197398	0.001859572	0.035769723	-1.489475025
SYNE1	0.831569963	10.35784061	3.708095736	0.000599987	0.01794018	-0.449748574
CAPG	0.800942969	12.58442574	3.18196661	0.002734181	0.043878408	-1.840890187
ETS2	0.798225644	12.16535358	4.14456854	0.000159074	0.008545486	0.782245861
PTPRK	0.797349045	11.21635797	3.468604215	0.001211954	0.027838934	-1.09733277
PTPN6	0.79593917	12.5256424	3.203864823	0.002572392	0.042686899	-1.785401626
EVL	0.778812276	12.04887992	5.160862841	6.14E-06	0.000845997	3.831957908
SIGIRR	0.778021549	11.10434562	4.988429703	1.08E-05	0.001243362	3.301920838
IRF2	0.776437125	11.19515046	3.197871565	0.002615747	0.042960758	-1.800610729
PTPRB	0.76267256	10.43687725	3.256540402	0.002219543	0.03952158	-1.651002465
MGLL	0.760570038	12.84976261	3.132966814	0.003131728	0.046820811	-1.964220228
EHD2	0.748478322	10.73237431	3.493395026	0.001127936	0.027186262	-1.031351342
BCL6	0.74333508	11.56427088	4.180659369	0.000142205	0.008121076	0.886707229
PACSIN2	0.74066435	14.66736076	4.245950227	0.00011601	0.007139707	1.076578008
SDC1	0.729332553	13.13652006	3.308694658	0.001915766	0.036157354	-1.516674514
NAV2	0.725285218	10.72181111	3.434810075	0.001336169	0.029512115	-1.186866033
RPS6KA2	0.721687854	11.31487378	3.873282673	0.000365395	0.013624942	0.009256919
ZYX	0.701574336	11.96696812	3.877728289	0.000360509	0.01360279	0.021738659
CASKIN2	0.69259258	11.47460521	3.941877995	0.000296672	0.012524094	0.202565341
S100A6	0.692055636	15.24190599	3.168374069	0.002839397	0.044435026	-1.875217839
CBX6	0.686781881	13.72433719	3.463586287	0.001229674	0.027838934	-1.110657244
C1RL	0.67278197	10.6985639	3.27736126	0.002093158	0.038237831	-1.597524941
MAN1A1	0.671761759	11.20082605	3.111045264	0.003326719	0.04881498	-2.019017939
MAFF	0.667334275	11.32940635	3.562614645	0.000921842	0.023658113	-0.845800885
CCNL1	0.663256263	13.58886675	3.887636775	0.000349846	0.013602304	0.049581651
CD59	0.635702318	15.20116589	3.406717343	0.001448595	0.030917989	-1.260928023
CTNNAL1	0.624316393	13.92797511	3.150077727	0.002987077	0.045407864	-1.921284694
CD151	0.604727126	13.54205172	3.164961782	0.002866405	0.044435026	-1.883821588
CAPN1	0.604352355	11.80907253	3.722347876	0.00057505	0.017732928	-0.410524464
WSB1	0.601391846	13.92219298	3.516607913	0.001054341	0.026312861	-0.969341658

(continued)

Table S2. (continued)

	logFC	AveExpr	t	*p v*alue	adj.*p* Val.	B
PLEKHF2	0.599853813	12.65770068	3.604905618	0.000814251	0.021618491	-0.731501242
ARF6	0.592494282	12.53170047	3.718645338	0.000581431	0.017791799	-0.420721501
CD81	0.592056009	15.39865127	3.40044661	0.001474894	0.030965196	-1.2774139
PAX1	0.586215867	11.38646478	3.376303315	0.001580467	0.032214075	-1.340729104
C2	0.584484047	13.12877375	3.172937	0.002803657	0.044354488	-1.863704122
LRRFIP1	0.572810914	12.97608061	3.736280287	0.00055164	0.017524386	-0.372109404
CAPN2	0.569951981	14.70508575	3.164579594	0.002869445	0.044435026	-1.884784888
WASF2	0.563377225	10.65914283	3.465695124	0.001222197	0.027838934	-1.105058767
MACF1	0.556624939	14.64016434	3.398610046	0.001482683	0.031018898	-1.282239072
PPM1F	0.550920294	13.34233215	3.3935661	0.001504275	0.031264263	-1.295483483
NCK2	0.546321035	11.7950244	4.028457489	0.000227636	0.010654432	0.448676762
VCL	0.545355914	14.21372169	3.548246205	0.000961406	0.024573996	-0.884474704
FLI1	0.538908371	11.96134622	3.133335862	0.00312854	0.046820811	-1.963295699
FTH1	0.524280797	17.0786338	3.521612014	0.001039089	0.026034736	-0.955945346
ARHGDIA	0.520681741	11.40292197	3.225596505	0.002420824	0.041031019	-1.730111203
H6PD	0.518538982	10.7467192	3.428004862	0.001362613	0.029887895	-1.204837605
PON2	0.518406725	13.84156249	3.75693222	0.000518622	0.017168321	-0.315039227
IRS2	0.517372627	10.92876909	3.300680418	0.001959727	0.036537373	-1.537396103
HK1	0.515594711	13.37926466	3.143049012	0.003045715	0.046188488	-1.938938706
LPP	0.513535752	12.66692186	3.965368036	0.000276156	0.012106595	0.269108673
BTG1	0.503196822	16.1012217	3.257165728	0.002215644	0.03952158	-1.649399238
STAT3	0.494566433	14.04116375	3.651551615	0.00070958	0.01971078	-0.604632474
RNF38	0.490812316	12.09084395	3.925926008	0.000311438	0.012737497	0.157475624
STAT6	0.445622754	12.22285788	3.246015765	0.002286151	0.04033898	-1.677958733
CDC42EP4	0.423372434	10.70985825	3.360533812	0.00165327	0.032852907	-1.381947776
GNAQ	0.386627058	12.99472037	3.105977733	0.003373396	0.049158517	-2.031651726
SET	-0.354570339	15.29504793	-3.353322194	0.001687618	0.033326516	-1.400761443
RPLP0	-0.362479769	18.06552824	-3.228856089	0.002398833	0.040767293	-1.72179898
IK	-0.363671215	13.87639243	-3.171704063	0.002813272	0.044361516	-1.866816196
SUCLG1	-0.363711899	13.60696245	-3.283116481	0.002059447	0.037840099	-1.582707941
EIF2S2	-0.373716302	14.4147489	-3.361751747	0.001647535	0.032852907	-1.378768178
DDOST	-0.37832271	15.41295615	-3.163255715	0.002879999	0.044435026	-1.88812117
SRP14	-0.396520474	15.48296024	-3.656214879	0.000699858	0.01958248	-0.591903938
RAD17	-0.409284046	12.59657159	-3.17558213	0.002783133	0.044327344	-1.857025055
PPP2CA	-0.410394934	14.69711418	-4.068015925	0.000201551	0.009752924	0.561882417
CSNK1G3	-0.412214419	11.76009943	-3.11987931	0.003246802	0.047867555	-1.996963668
CEBPZ	-0.414342829	13.82613976	-3.467628787	0.001215379	0.027838934	-1.099923713
HAT1	-0.421432228	13.96407366	-3.172658099	0.002805829	0.044354488	-1.864408164
PMS1	-0.426131934	12.84895229	-3.220595943	0.002454932	0.04127802	-1.74285342
BCAS2	-0.428619419	13.3474272	-3.307504931	0.001922232	0.036157354	-1.519752493
EIF2B4	-0.430514769	13.03341214	-3.440763931	0.001313437	0.029111452	-1.171126755
PWP1	-0.433521586	13.27839435	-3.234890128	0.002358622	0.040518447	-1.706398573
PSMA5	-0.434789622	14.21141317	-3.133923976	0.003123465	0.046820811	-1.961822233
GNPDA1	-0.437833036	12.69513163	-3.126199088	0.003190745	0.047363694	-1.981162773
SEPHS2	-0.449881232	13.68830471	-3.486679707	0.001150128	0.027305836	-1.049249308
GTF3C3	-0.450303211	13.28642076	-3.497391564	0.001114924	0.026975209	-1.020690832
PIGF	-0.452222823	13.70350759	-3.783867672	0.000478413	0.016280801	-0.240378391
PGAM1	-0.453162308	15.45629819	-3.298544116	0.001971606	0.036651054	-1.542914835

(continued)

Table S2. (continued)

	logFC	AveExpr	t	*p* value	adj.*p* Val.	B
ATOX1	-0.459428627	13.42898316	-3.289190855	0.002024426	0.037304762	-1.567052938
USP14	-0.468365276	12.32905291	-3.421543666	0.001388181	0.030135892	-1.221882549
ANAPC5	-0.469725335	13.9185076	-3.708886869	0.000598576	0.01794018	-0.447573185
RAD50	-0.470348137	12.68935659	-3.571423073	0.000898364	0.023339066	-0.822051998
CRADD	-0.470419017	11.16287692	-3.450375802	0.001277515	0.028612744	-1.145685931
RPL6	-0.472785676	16.80132214	-3.703653067	0.000607971	0.01795497	-0.461960405
LRPPRC	-0.475773436	13.92477622	-3.292673938	0.002004601	0.037047133	-1.558068716
RPL37	-0.476749679	18.83901934	-3.755957327	0.000520137	0.017168321	-0.317736683
RFC5	-0.479417317	10.86845821	-3.335418395	0.001775854	0.034637353	-1.447369941
COX6A1	-0.483745968	16.04677982	-3.15834854	0.002919441	0.04459359	-1.900480286
MRPL19	-0.483890723	13.3584571	-3.229255578	0.002396151	0.040767293	-1.720779905
DNM1L	-0.485040917	12.68447277	-4.168826427	0.000147534	0.008276272	0.852418543
TIMM44	-0.492362694	12.0560915	-3.22086551	0.002453082	0.04127802	-1.74216682
DENR	-0.495145452	14.53707683	-3.670291122	0.000671283	0.018986312	-0.553433026
DUT	-0.495304627	14.99871602	-3.307511559	0.001922196	0.036157354	-1.519735346
TBL2	-0.497368766	14.47144766	-3.156563677	0.002933914	0.044706922	-1.904972726
GTF3C2	-0.498013932	13.34574926	-3.814791857	0.000435957	0.015352968	-0.15434987
PPP1CC	-0.498223204	15.09755812	-3.471732873	0.00120103	0.027785872	-1.089019734
COPS5	-0.499689449	14.70297669	-3.33091315	0.001798739	0.03486914	-1.459076007
CDC27	-0.501012957	11.95561247	-3.532593897	0.001006357	0.025415514	-0.926510781
MRPL22	-0.506234703	14.11673691	-3.77690556	0.000488508	0.016471547	-0.25970066
TNPO1	-0.507284507	13.81447413	-3.500569344	0.001104681	0.026829776	-1.012209654
RNASEH1	-0.519616559	13.49179363	-3.512627667	0.001066625	0.026411458	-0.979989816
NDUFA8	-0.519743744	14.21413289	-3.735511904	0.000552907	0.017524386	-0.374229839
MRPL9	-0.523055692	14.06075297	-3.206307478	0.002554918	0.042508205	-1.779198027
AK2	-0.524731379	12.69240387	-3.348412881	0.001711388	0.033586661	-1.413555794
IMMT	-0.529750079	14.16836696	-4.321169065	9.16E-05	0.005867895	1.296688726
MRPS35	-0.530499289	12.69485201	-3.237441704	0.002341812	0.04033898	-1.6998812
NAPG	-0.532804702	11.91478292	-3.480546932	0.001170758	0.027588985	-1.065578484
UBA2	-0.532934117	14.02767534	-3.459545179	0.001244124	0.028065834	-1.121380293
EIF2B3	-0.534310537	13.45674606	-4.322715874	9.12E-05	0.005867895	1.301229975
GDAP2	-0.535112355	11.30887658	-3.309633997	0.001910675	0.036157354	-1.51424387
LSM3	-0.535604577	14.45567913	-3.754304965	0.000522714	0.017168321	-0.322307881
MRPS7	-0.538808319	12.59043745	-3.199996469	0.002600297	0.042925223	-1.795220299
COX5B	-0.540269118	13.30068364	-3.404611622	0.001457376	0.030950588	-1.266465881
HMBS	-0.541720392	12.0197992	-3.890819104	0.000346487	0.013602304	0.058530877
CAMLG	-0.54497199	13.00381613	-3.881312315	0.000356616	0.01360279	0.031806099
AFG3L2	-0.54562854	12.15892552	-3.139451696	0.003076145	0.046538627	-1.947964799
ACP1	-0.550242847	13.02037253	-3.267609518	0.002151477	0.038963723	-1.622596618
NOLC1	-0.55672801	12.30900819	-3.730586583	0.000561094	0.017607793	-0.387816769
PSMB7	-0.558915205	15.58327287	-3.638098742	0.00073836	0.020174419	-0.641306691
XRCC5	-0.56272717	15.49253076	-4.212793289	0.000128663	0.007482534	0.980013637
ARSB	-0.563063574	10.31369627	-3.245844838	0.002287249	0.04033898	-1.678396098
PSMA2	-0.565434899	14.91607441	-3.685570184	0.000641537	0.018485017	-0.511591404
FANCL	-0.566261686	13.31029264	-3.308505653	0.001916792	0.036157354	-1.517163535
MSH2	-0.57308921	13.71428064	-4.428587004	6.53E-05	0.004813311	1.613417751
CDK5RAP2	-0.581087892	11.01517836	-3.627889052	0.000760948	0.020702349	-0.669093894
PCNA	-0.581946428	14.50776844	-3.160622003	0.002901105	0.04459359	-1.894755828

(continued)

Table S2. (continued)

	logFC	AveExpr	t	*p* value	adj.*p* Val.	B
BRD8	-0.585661868	13.02911625	-3.926480807	0.000310913	0.012737497	0.15904245
CCT5	-0.590978412	15.72463566	-3.160055207	0.002905666	0.04459359	-1.896183221
ZZZ3	-0.591300982	12.43952712	-3.9119353	0.000324973	0.013121049	0.117996664
CHCHD3	-0.591858803	13.9731541	-3.208467617	0.002539559	0.042363848	-1.77370959
PREB	-0.594395419	14.24379416	-3.721636337	0.000576271	0.017732928	-0.412484472
HSPA4	-0.595799693	14.38811935	-3.728540957	0.000564528	0.017610649	-0.393457246
LSM5	-0.603580359	13.06914601	-3.242561754	0.002308421	0.04033898	-1.686794173
GSTM3	-0.604571402	12.57891478	-3.604557823	0.000815084	0.021618491	-0.732444062
WDR12	-0.604875167	13.02265435	-3.36213868	0.001645717	0.032852907	-1.377757897
LARS2	-0.6050181	12.10059743	-5.078477927	8.04E-06	0.001061818	3.578250821
PSMD14	-0.607957834	15.15553583	-4.339178676	8.66E-05	0.005720479	1.349599146
MRPS12	-0.608803865	12.39103908	-3.952602954	0.000287128	0.01233854	0.232925798
FANCG	-0.615933527	12.10653705	-3.842701404	0.000400784	0.01443506	-0.076426657
CCT7	-0.616298102	15.59852892	-3.645902566	0.000721531	0.019886034	-0.620040798
PRMT3	-0.617242106	11.47775741	-3.613292316	0.000794398	0.02124762	-0.708752143
BTF3	-0.619570636	14.83030057	-3.279328329	0.002081577	0.038136181	-1.592462354
CCT2	-0.62039787	14.9445237	-3.295503512	0.001988632	0.036859461	-1.550766107
PDCD2	-0.624069201	11.13485151	-3.266620009	0.00215748	0.038963723	-1.62513821
DDX1	-0.625016049	14.83200322	-4.409466559	6.94E-05	0.004941143	1.556841855
PFN2	-0.627558026	12.98509466	-3.125799724	0.00319426	0.047363694	-1.982161852
THAP10	-0.62839597	11.44610142	-3.242222903	0.002310617	0.04033898	-1.687660665
CYCS	-0.634232685	15.95882023	-3.655543515	0.00070125	0.01958248	-0.593736949
RPE	-0.634762157	11.98355477	-3.305177449	0.001934942	0.036181705	-1.525772153
COX7C	-0.635720065	15.60355066	-3.166650959	0.002853005	0.044435026	-1.879563194
CSE1L	-0.636179373	14.05399463	-3.885266331	0.000352369	0.013602304	0.042917734
RPL26L1	-0.636424564	14.49445351	-3.731229346	0.000560019	0.017607793	-0.386044143
SLC30A5	-0.63843023	12.64434987	-4.713729623	2.63E-05	0.002252694	2.466336053
ATIC	-0.638754407	13.97026545	-3.41790239	0.001402792	0.030349135	-1.231480607
CDK7	-0.639400666	12.66377369	-3.671770256	0.000668346	0.018986312	-0.549386206
GEMIN6	-0.642932309	12.67483082	-3.104125521	0.00339061	0.049183238	-2.036266284
EEF1E1	-0.645403029	12.75439418	-3.389202707	0.001523196	0.031408045	-1.306932061
NDUFS1	-0.647298827	13.50026931	-3.879467142	0.000358616	0.01360279	0.026622524
POP5	-0.650436296	13.3793339	-5.494171947	2.05E-06	0.000418637	4.865526803
NDUFS6	-0.650705103	12.36264308	-3.506741522	0.001085042	0.02662895	-0.995724972
MTHFD1	-0.650830071	14.22241285	-3.717281749	0.000583798	0.017791799	-0.424475667
CCT3	-0.652709859	15.0903824	-3.169008668	0.0028344	0.044435026	-1.873617144
SNRPD1	-0.653857325	12.88664299	-4.1631216	0.000150172	0.008277755	0.835901161
MRPS18B	-0.655897044	12.51492277	-3.988054262	0.000257653	0.011583417	0.333538606
GLMN	-0.656538838	10.95877345	-3.505801709	0.00108801	0.02662895	-0.998236029
NDUFB3	-0.656898188	11.58766938	-4.526920668	4.78E-05	0.003786315	1.905665112
MRPS27	-0.658748915	13.15536372	-3.567005637	0.000910066	0.023450837	-0.833965906
VRK1	-0.663551336	11.97516011	-3.843143315	0.00040025	0.01443506	-0.075190726
IDH3B	-0.677708303	13.1333191	-4.092461848	0.00018691	0.00929555	0.632069819
ASB6	-0.678988099	11.24078202	-3.333897304	0.00178355	0.034680741	-1.451323229
PPIC	-0.680259809	15.01100585	-3.932963578	0.000304838	0.012712939	0.177357948
DCP2	-0.684888426	12.53142319	-3.682347773	0.000647703	0.018578233	-0.520423142
MRPS15	-0.685607271	12.86479863	-3.835769147	0.000409255	0.014656892	-0.095806106
MRPL12	-0.687658464	12.95346602	-3.650370454	0.000712063	0.01971078	-0.607855195

(continued)

Table S2. (continued)

	logFC	AveExpr	t	*p value*	adj.*p* Val.	B
RIOK2	-0.688118578	11.93986427	-4.884550435	1.51E-05	0.001571619	2.984547189
NRAS	-0.688479244	12.03068594	-3.874442422	0.000364114	0.013624942	0.012512459
SLC5A6	-0.693221124	11.86682396	-3.182238677	0.002732113	0.043878408	-1.840202186
LCMT2	-0.695177396	11.17701238	-3.185198103	0.002709715	0.043878408	-1.832716138
TAF1B	-0.695610627	11.17302334	-5.591705355	1.48E-06	0.000335566	5.169673924
PPM1G	-0.699495768	12.69484444	-6.063243037	3.09E-07	0.000103128	6.646278807
AKR7A3	-0.7028833	10.59304067	-3.312340326	0.00189608	0.036157354	-1.507238736
FEN1	-0.704280043	13.73317675	-3.257082351	0.002216163	0.03952158	-1.649613013
PAX3	-0.704452422	9.713888927	-3.208782238	0.002537329	0.042363848	-1.772910024
RPA3	-0.707195512	12.30865333	-4.800024614	1.99E-05	0.001939369	2.727517775
MCTS1	-0.707722473	13.57048885	-3.887681827	0.000349798	0.013602304	0.049708323
DNAJC10	-0.713126849	12.2144711	-4.071880672	0.000199165	0.009711568	0.572967036
MRPL35	-0.713447389	12.28948605	-3.163127733	0.002881022	0.044435026	-1.888443651
PIGK	-0.713884076	12.13252549	-3.104143746	0.00339044	0.049183238	-2.036220887
MTIF2	-0.714294867	11.84581592	-4.53840651	4.61E-05	0.003696435	1.939936803
CRIPT	-0.719860747	11.29740048	-3.357279066	0.001668689	0.033055679	-1.390441579
STOML2	-0.721952703	14.51957697	-4.392983343	7.31E-05	0.00509097	1.508136903
PLK1	-0.722243572	13.08977063	-3.253108058	0.002241061	0.039792951	-1.659799186
ITGB3BP	-0.728403841	13.53590625	-3.805789814	0.000447926	0.015601098	-0.179426846
FHIT	-0.730633954	9.826248561	-3.183845762	0.002719928	0.043878408	-1.836137486
TTF2	-0.730841167	11.37004038	-4.422992525	6.65E-05	0.004842999	1.596855477
RPP40	-0.73429784	12.06272878	-3.119851599	0.00324705	0.047867555	-1.997032908
KPTN	-0.737620154	10.37097751	-3.384157607	0.001545355	0.031702291	-1.320159044
RAN	-0.748254834	14.93260131	-4.110761987	0.000176633	0.009177651	0.684724691
UROD	-0.752654219	14.22062184	-4.339042693	8.66E-05	0.005720479	1.349199344
PFKM	-0.762656971	12.84816761	-3.447430949	0.00128842	0.028657166	-1.153484522
MCM6	-0.768864931	14.22600759	-3.995867175	0.000251564	0.011390438	0.355764454
HUS1	-0.771619339	11.22543749	-3.969050001	0.000273068	0.01210474	0.279554755
USP39	-0.772188399	12.6183139	-3.741792108	0.000542635	0.017524386	-0.35689274
MTX1	-0.779545254	13.50975667	-4.130253085	0.000166291	0.008841053	0.740911084
UQCRFS1	-0.781810415	14.35819869	-3.389487425	0.001521954	0.031408045	-1.306185272
CDC7	-0.787718703	12.24958858	-3.796220596	0.000460995	0.015968582	-0.206053222
PRDM5	-0.790295583	10.79033153	-4.487876406	5.41E-05	0.004182614	1.78937315
CDC23	-0.790555065	12.987651	-5.403680366	2.76E-06	0.000501128	4.583942705
RAPGEF3	-0.794435911	9.293932488	-3.182594546	0.00272941	0.043878408	-1.839302215
RFC3	-0.79529586	11.71846309	-4.036408292	0.000222143	0.01058768	0.471392489
HSPD1	-0.807865034	15.35214087	-3.819277901	0.000430109	0.015231635	-0.141842744
MRPL13	-0.809561459	13.69032238	-3.125654262	0.003195542	0.047363694	-1.982525734
NPM3	-0.812719966	11.88781153	-3.238700108	0.002333563	0.04033898	-1.696665805
ARTN	-0.827805555	9.811908263	-3.262195291	0.002184519	0.039228511	-1.636497775
CETN3	-0.827981404	12.59434749	-4.522117719	4.85E-05	0.00379722	1.891342192
TOE1	-0.829024107	10.733632	-4.220206096	0.000125723	0.007381284	1.001577164
RACGAP1	-0.833465238	12.79048287	-3.787439031	0.000473313	0.016218013	-0.230460075
SHMT2	-0.837519665	13.09740507	-3.922123798	0.000315061	0.012802398	0.14674033
PHB	-0.837627706	13.34604503	-4.730125022	2.49E-05	0.002252694	2.515858609
PTTG1	-0.841328939	12.76551543	-3.77406467	0.000492686	0.016524524	-0.267580244
CAD	-0.842742076	13.06818125	-3.957731734	0.00028267	0.012272904	0.247457281
SHCBP1	-0.842778513	12.61350359	-3.463866274	0.001228678	0.027838934	-1.10991405

(continued)

Table S2. (continued)

	logFC	AveExpr	t	*p value*	adj.*p* Val.	B
CDT1	-0.863586956	10.46409857	-3.18331327	0.00272396	0.043878408	-1.83748442
NUP155	-0.86654374	12.10813778	-3.864882984	0.000374802	0.01388348	-0.014308635
DHX57	-0.874563111	10.17146161	-3.47362491	0.001194469	0.027754789	-1.083990509
AHCY	-0.87993741	15.28000037	-4.811009158	1.92E-05	0.001900941	2.760854759
EXO1	-0.881287479	11.90965538	-4.027101847	0.000228585	0.010654432	0.444805535
SIRT4	-0.883172245	9.481523584	-3.263318844	0.002177623	0.039215767	-1.633614131
SPAG5	-0.885117832	11.92470002	-3.622152937	0.000773928	0.020787833	-0.684688202
DLL3	-0.90541138	9.733141123	-3.243298051	0.002303657	0.04033898	-1.684911171
EXOSC5	-0.911344601	12.04567062	-3.859382063	0.000381089	0.01388348	-0.02972892
KIF11	-0.917121759	12.43862065	-3.407507896	0.001445311	0.030917989	-1.25884845
SARS2	-0.918546385	10.04028975	-3.388547294	0.001526057	0.031408045	-1.30865101
TUFM	-0.938130135	14.08860985	-5.880194117	5.69E-07	0.000171626	6.07222189
CDC25C	-0.945405838	10.89865105	-4.744785924	2.38E-05	0.002183591	2.560182479
ENDOG	-0.981228832	10.55287714	-3.513447642	0.001064083	0.026411458	-0.977796701
NUSAP1	-0.988618413	13.39596039	-3.668972771	0.000673911	0.018986312	-0.557039264
MRPL42	-0.992675235	12.33939895	-5.378601868	3.00E-06	0.000513843	4.506020929
THOP1	-0.998671642	11.43576457	-3.887604888	0.00034988	0.013602304	0.049491996
NUDT1	-1.001320311	12.96168309	-4.086620513	0.000190312	0.009351825	0.615282838
ATAD2	-1.014488252	12.12216687	-3.275424231	0.002104621	0.038336764	-1.60250849
ADAMTS5	-1.029814689	12.96174887	-3.134174378	0.003121307	0.046820811	-1.961194822
KIF4A	-1.034282186	12.32986301	-3.338704002	0.001759339	0.034421149	-1.43882721
NEK2	-1.053123998	11.91841379	-3.638820856	0.000736787	0.020174419	-0.639339852
TYMS	-1.077255632	15.0370618	-4.40462534	7.04E-05	0.004961608	1.542530388
ITGA4	-1.086847188	12.39770451	-3.487044288	0.001148912	0.027305836	-1.048278085
RAD51	-1.11271807	11.95493429	-3.426092984	0.001370131	0.029896962	-1.209883074
OIP5	-1.125761756	10.87985693	-4.914350025	1.37E-05	0.001475033	3.075429213
MELK	-1.130332406	12.80125484	-3.713507118	0.000590399	0.01788758	-0.434864281
DHFR	-1.143019247	12.24995316	-5.285622244	4.07E-06	0.00061498	4.217607356
CCNB2	-1.150326763	12.86928841	-3.859411768	0.000381055	0.01388348	-0.029645678
BUB1B	-1.166377525	10.98251245	-3.736838644	0.000550721	0.017524386	-0.370568424
HSD17B1	-1.193289141	9.25748613	-3.501327686	0.00110225	0.026829776	-1.010185105
TRIP13	-1.195964525	12.30054791	-4.713397582	2.63E-05	0.002252694	2.465333614
TOP2A	-1.198776902	14.23888963	-3.467182608	0.001216949	0.027838934	-1.101108727
MAD2L1	-1.203586775	14.2780341	-3.402174528	0.001467602	0.030965196	-1.272872854
QPRT	-1.333220301	10.1075211	-3.229277514	0.002396003	0.040767293	-1.720723945
MYBL2	-1.335261639	10.32885443	-4.128174935	0.000167365	0.008841053	0.734915356
KIF20A	-1.338788763	12.52054406	-4.204767046	0.000131923	0.007602356	0.956682112
EGF	-1.401033098	8.429009023	-3.404011619	0.001459887	0.030950588	-1.26804349
CCNB1	-1.401435911	13.44387938	-4.414600759	6.83E-05	0.004916801	1.572025323
HMMR	-1.445195138	11.6599248	-5.351732835	3.28E-06	0.000546379	4.422595447
RAD54L	-1.634391282	9.699032486	-5.46486046	2.26E-06	0.000446837	4.774249561
KCNK2	-1.794962636	9.258758678	-4.479672384	5.55E-05	0.00424135	1.764979484
THBS4	-2.056243723	11.0900658	-4.106783963	0.000178819	0.009215709	0.673270601
MYL1	-2.136798844	9.013718234	-3.237840555	0.002339194	0.04033898	-1.698862162
MMP13	-2.398819444	12.95995122	-3.193867323	0.002645098	0.043326303	-1.810762828

Table S3. The expression levels of 8 prognostic genes of GSE14359, GSE32981, and TARGET database

	logFC	AveExpr	t	*p* Value	adj.*p* Val	B
ISLR	1.516135301	11.35174028	4.008266723	0.000242185	0.011203013	0.39107654
MFAP4	2.497812562	11.18533685	4.231041881	0.000121542	0.00726842	1.033124087
KIFC3	0.901054965	12.0293576	3.107972109	0.003354952	0.049002403	-2.026681088
MAOB	1.133608705	10.96669401	3.158801514	0.002915779	0.04459359	-1.89933992
EGR1	1.745012312	14.36706334	6.590499255	5.34E-08	3.38E-05	8.299761149
FOS	2.483668532	15.58785497	6.230861802	1.77E-07	6.59E-05	7.172257246
FBP1	1.73847279	10.95046109	4.164520092	0.000149521	0.008277755	0.839949438
ANK3	0.928508677	9.81622411	3.372571875	0.001597412	0.032438236	-1.35049221

Table S3.1. The expression levels of 8 prognostic genes of GSE14359

	GSM359139	GSM359140	GSM359143	GSM359144	GSM359147
ISLR	9.249587556	9.533329732	10.4427362	10.09776879	9.34251919
MFAP4	7.899054756	8.662846365	8.653561662	6.537606691	11.20951429
KIFC3	8.342963574	9.445014846	9.745506266	9.807515928	10.37764436
MAOB	9.617467465	9.77939106	8.560332834	9.229299509	10.42227506
EGR1	11.14386148	11.22439366	12.3328198	12.23060592	11.29737486
FOS	12.3632587	12.30865188	13.3240258	12.81360084	11.58730873
FBP1	11.08101733	10.64961546	9.884475819	10.31650782	8.799605422
ANK3	10.33862497	10.38136269	8.999718196	9.434141688	10.1822288

Table S3.2. The expression levels of 8 prognostic genes of GSE32981

	GSM816950	GSM816958	GSM816960	GSM816961	GSM816964
ISLR	13.54733562	15.51218319	11.63838863	12.33459568	9.605576515
MFAP4	18.2706604	14.28722763	10.03917313	12.95284748	9.290056229
KIFC3	13.75560284	12.18449593	12.58251762	12.95044994	15.11413002
MAOB	11.05630207	11.0048275	12.08586025	11.73992634	9.651494026
EGR1	14.02221584	14.33392811	15.37380981	15.72906303	14.04688168
FOS	16.14503288	15.83769894	14.51157665	17.46303177	14.29434967
FBP1	10.44786644	11.54994774	9.786218643	8.860423088	10.36763573
ANK3	8.558703423	7.242418289	11.30948544	7.449539661	10.72542858

Table S3.3. The expression levels of 8 prognostic genes of TARGET database

	TARGET-40-0A4HLD-01A	TARGET-40-0A4HMC-01A	TARGET-40-0A4HX8-01A	TARGET-40-0A4HXS-01A	TARGET-40-0A4I0W-01A
ISLR	5.944003349	7.733229591	8.017056699	1.952594495	4.039849036
MFAP4	3.241977431	2.688359425	8.075823537	2.471733734	6.416773887
KIFC3	3.058645524	3.457686214	1.956577119	2.088141597	1.892157844
MAOB	1.196921734	0.876880337	0.100304906	1.02219024	1.21549223
EGR1	8.061519168	6.343594366	4.945701333	3.379218925	5.89011103
FOS	7.692770311	6.842854413	2.964638907	2.579711163	2.627326676
FBP1	1.070183214	2.860784063	1.234194723	1.42921423	1.63371019
ANK3	0.507617067	0.45995614	0.977316563	0.154842407	0.116497841

Table S4. The expression levels of 8 prognostic genes for each sample from RT qPCR experiment

	Samples	Mean	standard deviation	*p* value	log2FC
ANK3	MNNG/HOS CI	1.016059	0.229493		-3.503371713
	143B	0.089598132	0.020269922	0.002233511	
EGR1	MNNG/HOS CI	1.028110169	0.303844371		-7.9507484
	143B	0.004155525	0.000302495	0.004293929	
FBP1	MNNG/HOS CI	1.067486654	0.496193344		5.814668434
	143B	60.0830634	4.028384129	1.47602E-05	
FOS	MNNG/HOS CI	1.014223953	0.215502583		-7.785025349
	143B	0.004598417	0.000702962	0.001254144	
ISLR	MNNG/HOS CI	1.046483582	0.400104753		2.804301802
	143B	7.087523574	1.340125552	0.00170677	
KIFC3	MNNG/HOS CI	1.036858743	0.355180397		-3.159883288
	143B	0.325386879	0.039740135	0.026102004	
MAOB	MNNG/HOS CI	1.01142197	0.19048492		-1.444268682
	143B	0.37167572	0.107955555	0.007176211	
MFAP4	MNNG/HOS CI	1.083663002	0.513585881		2.799760186
	143B	6.963246936	1.716206094	0.004727439	